Title
ALPHA DECAY: A SURVEY

Authors
Rasmussen, J.O.
Perlman, I.

Publication Date
1963-02-01

UCRL-10669

University of California

Ernest O. Lawrence Radiation Laboratory

ALPHA DECAY: A SURVEY

DISCLAIMER

For book by K. Siegbahn, "Alpha Beta & Gamma Spectroscopy"

UCRL-10669
(corrections made)

UNIVERSITY OF CALIFORNIA

Lawrence Radiation Laboratory
Berkeley, California

Contract No. W-7405-eng-48

ALPHA DECAY: A SURVEY

J. O. Rasmussen and I. Perlman

February, 1963

ALPHA DECAY: A ~~REVIEW~~ SURVEY

J. O. Rasmussen and I. Perlman

Department of Chemistry and Lawrence Radiation Laboratory
University of California
Berkeley, California

February, 1963

1. Introduction

Alpha radioactivity has in recent years yielded much invaluable energy level information to the nuclear spectroscopist. The sharp, monoenergetic character of alpha radiation (like gamma radiation) and its charged-particle nature (like beta radiation) make possible precision spectroscopy by large magnetic spectrographs down to line widths of a few keV. Lower resolution spectroscopy, but with high geometry, is performed often with ionization chambers and solid-state semiconductor detectors. Scintillation-photomultiplier detectors also find use for alpha detection, though energy discrimination is not so good as with other methods.

Alpha transitions, in sharp contrast to beta and gamma transitions, are only mildly inhibited by angular momentum changes, and are thus more likely to populate in detectable intensity all the low-lying states of the daughter nucleus. As a spectroscopic tool, the alpha radiation suffers from two main restrictions. First, it is limited to certain regions of nuclei, the largest encompassing the trans-lead nuclei, another consisting of rare-earth nuclei with 84 and a few more neutrons. There are a few scattered cases found among the neutron-deficient nuclei between these two regions. The second main restriction is that alpha transition rates exhibit an extremely sensitive exponential energy dependence on decay energy, so that in practice only states up to a few hundred kilovolts excitation are excited in alpha decay. We may point out also a few cases where some alpha radiation

arises from excited nuclear states following beta decay (i.e. Li^8, B^8, B^{12}, N^{12}, Na^{20}, Al^{24}, Cl^{32}, Bi^{212}, and Bi^{214}).

In the trans-lead region, where alpha decay is so prevalent, the Q-values of alpha and beta decay have been used to calculate relative atomic masses within the four connected families whose mass numbers are of form 4n, 4n+1, 4n+2, and 4n+3. When supplemented by three nuclear reaction Q values, the families are linked together to give atomic masses over the whole heavy region [1,2].

In addition to the above-mentioned interests deriving from energy measurements, the alpha decay rates and "fine-structure" intensity patterns are interesting in their own right. The predominant factor governing alpha decay rates, the Coulombic barrier penetration, has long been recognized[3,4], and there have been many attempts to derive nuclear size or shape information therefrom[5]. It is only recently that the more subtle connections with the powerful concepts of the nuclear shell models are becoming clear. In this introduction we will mention only the one shell-model rate concept for odd-mass nuclei that has been recognized the longest and that has played such an important role in establishing the Nilsson orbital assignments to rotational bands of the spheroidal odd-A heavy nuclei. This concept is that the rotational band of the daughter nucleus in which the orbital of the odd nucleon is the same as in the parent will be intrinsically "favored" by the alpha decay and will exhibit reduced transition rates (the word "reduced" signifying that the Coulombic barrier penetrability factor has been divided out) nearly as great as the neighboring even-even nuclei. Decay to all other bands will show lower reduced rates. The even-even nuclei of the heavy region exhibit very uniform reduced transition rates to their ground states, except for a drop of an order of magnitude in going to nuclei with 126, or less, neutrons.

The problem of relative intensities to states in the same rotational band is strongly connected to the problem of alpha wave penetration through the anisotropic barrier surrounding the spheroidal nucleus. We will return in a later section to the problems of rate theory, trying to emphasize and develop simpler approximate methods and ideas, using as a guide and check the numerical calculations in the literature.

We must apologize in advance that to conserve space our literature referencing will be minimal and not properly representative of the important contributions that have developed alpha decay experiment and theory to its present state. We shall attempt primarily to include concepts and theoretical formulas useful to present-day research in alpha decay.

2. Alpha Decay Conservation Laws

The alpha decay process for bare nuclei has the equation

$$(Z + 2)^{A+4} \longrightarrow Z^{A} + {}_{2}He^{4}$$

Conservation of mass-energy requires that at infinitely large separation distance of the products the effective kinetic energy Q_f of the final system be given by the difference of rest masses of the nuclei times the square of the velocity of light

$$Q_f = (M_{A+4} - M_A - M_{He})\, c^2 \qquad (2.1)$$

The Q values for nuclear alpha decay rarely exceed 0.25% of the reduced mass, M_α ($= \dfrac{M_{He} + M_A}{M_{He} + M_A}$). Hence, non-relativistic treatments may be confidently employed.

Conservation of linear momentum then requires that the total kinetic energy be divided between the two products in inverse proportion to their masses.

The quantity Q_f is desired for careful theoretical treatment of alpha decay rates, but the Q value actually directly measurable in the laboratory is somewhat different, since one actually deals with atoms possessing a cloud of orbital electrons. The simple two-body break-up expressed by the equations above is an idealization to be inferred from a many-body problem with the electrons in the system. Because the electrons are so much lighter than the nuclear bodies, their presence does not usually make for difficulties in inferring properties of the decay process of the bare nuclei. A notable exception seems to be angular correlation experiments with alpha radiation; even when the daughter nucleus is in a vacuum the attenuation of the correlation is likely to be severe, indicating that the electrons of the daughter are left in configurations with unpaired electrons that produce magnetic fields or electric field gradients at the nucleus. Let us consider hypothetically that we have an assembly of bare nuclei of a given alpha emitter. As we feed orbital electrons into the system we would note almost no change in decay rate (possibly a very slight increase by virtue of the slight fraction of an electron charge lying within the barrier region, which extends to 3-5 times the nuclear radius). We would note a decrease in the alpha particle energy of 30-40 keV for heavy elements. This energy may be thought of in either of two nearly equivalent ways, as the work the alpha particle must do against the attractive Coulomb force of the electrons, or as the loss in total electron binding energy in going from a nucleus of charge Z+2 to one of charge Z. The exact amount of energy will be slightly lower in the sudden approximation, where the electron wave functions are assumed not to change, than in the adiabatic approximation, where the electron wave functions smoothly change to minimize the total energy as the alpha particle moves out[6]). For the three innermost shells the adiabatic approximation is

more appropriate and for the outermost two shells with binding energies well under 1 keV the sudden approximation is more appropriate, and a fair probability of ionization of valence electrons is expected.

The appropriate quantity for atomic mass calculations we will designate as Q with no subscript, and it is defined by an equation identical to eq. (2.1) except that the masses of the neutral atoms replace the nuclear masses. What would we observe with infinitely thin sources in a very high resolution magnetic spectrograph? We should observe no alpha decay events at all with energy release within 80 ev of Q, since this is the binding energy of electrons in He^4 and the alpha must have been doubly ionized to have been measured in the magnetic spectrograph. On the average one expects to lose an additional 70 ev (estimate for 4.5 MeV alpha from thorium) of the adiabatic energy to excitation and ionization. One should add about 150 ev to the apparent laboratory Q value to get the real Q value. The Q_f value may be inferred from the measured Q value by adding the "screening correction"

$$\Delta E_{SC} = 65.3\ Z_i^{7/5} - 80\ Z_i^{2/5}\ \text{ev} \qquad (2.2)$$

where Z_i is the atomic number of the parent.

In applying the laws of conservation of angular momentum and parity it is appropriate again to consider the two-body break-up of the bare nuclei and neglect the orbital electrons. As we have mentioned before, the electrons make their presence felt in attenuating angular correlations, essentially breaking down the conservation of the projection of nuclear angular momentum along a space-fixed axis.

The parity and the total angular momentum and its projection along an axis should be the same for the final system as for the initial parent nucleus. Since tha alpha particle is spinless and has even parity, the selection rules

assume an especially simple form. Namely, the orbital angular momentum of alpha decay is restricted to values between the sum and difference of initial and final spins.

$$| I_i - I_f | \leq L \leq I_i + I_f$$

If the parity of parent and daughter are the same, only even values of L are permitted; if opposite, then only odd values of L are permitted. The conservation of the projection of angular momentum may be expressed in terms of the magnetic quantum numbers. This conservation is relevant to angular correlation experiments.

If parent (or daughter) has spin zero, then certain spin and parity combinations of the daughter (or parent) states will be absolutely forbidden to the extent that parity is conserved in strong interactions. The orbital electrons could also mix in states causing violation of this selection rule, but their amplitudes would be of the order of the ratio of magnetic hyperfine energies to the separation energy of the admixed nuclear states.

The approximate selection rules appropriate to alpha decay will be discussed in a later section after development of decay-rate theory.

3. Decay Energies and Spectra of Alpha Emission

The discrete energetic nature of the two-body break-up that is alpha decay has facilitated accurate measurement of relative masses of nuclides throughout the whole trans-lead region. From knowledge of many alpha and some beta decay energies the relative masses within the four mass families ($4n$, $4n+1$, $4n+2$, $4n+3$) are calculable. It follows also that many unmeasured beta decay energies can be calculated from the energy balance of the closed cycles of alpha and beta decay energies. Figures 3.1 and 3.2 give such closed cycles. The alpha decay energies exhibit such smooth dependence on

mass number that they have been extrapolated to many unknown nuclei in the figs. 3.1 and 3.2. The general behavior of alpha-decay energies may be seen from a plot against mass number (fig. 3.3). The energies decrease for a series of isotopes with increasing mass number except for a large discontinuity at the major shell of 126 neutrons and a small discontinuity at a subshell of 152 neutrons.

The zig-zag nature of the line for uranium isotopes, where the odd-mass isotopes have energies less than the average of even-even neighbors, shows that the neutron pairing energy is decreasing from thorium to uranium. The zig-zag is of an opposite sense for especially elements 85 and 86, showing a neutron-pairing energy increase with increasing atomic number in this region.

Although nuclear mass measurements indicate that most naturally occurring nuclei of mass above ~150 are energetically unstable toward alpha emission, the process has been detected for only a few such nuclei below lead. The decay energies available to alpha emission drop so sharply below doubly magic Pb^{208} that the barrier penetrability factor pushes lifetimes into the region of $> 10^{16}$ years and beyond practical detectability. The exceptions that have been detected are listed in table 3.1.

Table 3.1

Naturally Occurring Alpha Emitters Below Lead[7)]

Isotope	Alpha Particle Energy (MeV)	Half-Life	Natural Isotopic Abundance
Pt^{190}	3.11±0.03	6.9×10^{11} y	0.012%
Hf^{174}	2.50±0.03	2.0×10^{15} y	0.18%
Gd^{152}	2.14±0.03	1.1×10^{14} y	0.20%
Sm^{147}	2.23±0.02	1.15×10^{11} y	14.97%
Nd^{144}	1.83±0.03	2.4×10^{15} y	23.85%

The systematic behavior of alpha decay energies for a series of isotopes is to increase as one moves from the beta-stable to the neutron-deficient region. The systematic behavior is interrupted by a discontinuity at closed shell configurations. It might be expected that some of the artificial neutron-deficient species near the isotopes of table 3.1 might exhibit detectable alpha decay, and this is indeed observed. Figure 3.4 plots the alpha decay energies of alpha emitters below lead vs. nuclear charge.

Higher resolution alpha-spectroscopic measurements have revealed complex structure in most of the trans-lead alpha emitters. As yet the measurements on sub-lead emitters have not been sufficiently sensitive to reveal fine structure.

The alpha decay of Po^{211} and Po^{211m} populate the low shell-model neutron-hole states in $Pb^{207}(p_{1/2}, f_{5/2}, p_{3/2}, i_{13/2})$. Likewise Bi^{211} populates the proton-hole states $s_{1/2}$ and $d_{3/2}$ in Tl^{207}. Nearby odd-odd nuclei populate the multiplet levels expected from coupling an odd proton and odd neutron in the spherical shell model. The odd-mass alpha emitters show mainly simple emission to ground for a few mass numbers above 211, then from ~219 to 229 the spectra show a great complexity that has not appreciably yielded to analysis in terms of nuclear models. For still heavier emitters the spectra continue to show many groups, but these complex spectra have largely been interpretable in terms of rotational bands based on states of the odd nucleon in the Nilsson model. The alpha decay spectral information has been of the greatest importance in establishing Nilsson orbital assignments[8,9] to ground and excited bands of the odd-mass deformed nuclei.

If we turn to the even-even nuclei, we find that the ground-state decay group is always the most intense. Decay to the first excited 2+ state is usually detectable, becoming more prominent as the energy of the state

drops in moving away from doubly-magic Pb^{208}. In contrast to the odd-mass nuclei, the excited energy levels, and consequently the alpha spectra, of even-even nuclei have smooth trends from nucleus to nucleus. Figure 3.5 displays the energy ratios and differences of excited states of even-even nuclei, most of which have been measured by alpha spectroscopy.

The usual alpha-emission data provide extensive information on decay rates from ground states of nuclei. In the light nuclei nuclear reaction data provide some alpha-emission widths from excited states. Also the (n,α) reaction has been detected[10]) with thermal neutrons for nuclei as heavy as Nd^{143} and Sm^{149}, giving some information on emission from states of several MeV excitation. We would be totally ignorant of alpha decay rates from lower excited states of heavy nuclei were it not for a curious occurrence observed following beta decay of Bi^{212} and Bi^{214}. Their beta transitions populate a number of excited levels in their respective polonium daughter nuclei, and the alpha decay energies from these excited states are so high that there occurs weak but detectable alpha radiation of high energy in competition with gamma de-excitation. The relative intensity of the long-range alpha groups can be used to fix the ratio of alpha to gamma widths of some of the excited states. Some of the earliest estimates[11]) of excited-state lifetimes were made from such data, together with alpha decay rate theory. The assumption was made that reduced alpha widths are the same for excited and ground states. Recent theoretical calculations of reduced alpha widths of excited states of Po^{212} show them to be substantially smaller than the reduced width from ground[12]). Thus, excited-state lifetimes calculated under the assumption of equal reduced widths must be lengthened in all cases.

4. Treatment of Alpha Decay Data

In this section we briefly summarize the ways in which alpha decay data may be treated.

Alpha energy determinations are usually made by interpolation between standards, based ultimately on a few alpha emitters measured in 180° uniform field magnetic spectrographs.

Most of the alpha decay energies in the literature are based directly or indirectly on standards listed by Briggs[13]). More recent determinations of Po^{210} seem to indicate a small but significant discrepancy in the older standardization. C. P. Browne summarizes the matter[14]) by saying that the Po^{210} alpha energy appears to be about 0.1% higher than the older accepted value. If such is the case, most of the published alpha decay energies are subject to increases of this percentage.

It is essential to use extremely thin sources in careful alpha spectroscopic work, since the rate of energy loss in matter is large. In studying weak groups in the presence of much stronger alpha groups it is important to minimize scattering from collimators, pole faces, backing, or support structures by careful design.

In the best work with magnetic spectrographs pains are taken to provide the thinnest possible sources and backing. Small-angle scattering from pole faces may be minimized by lining with a light element material, such as, beryllium. Penetration through the edges of collimators may better be minimized by using a heavy metal, such as tantalum. A good discussion of such considerations has been given by Walen and Bastin-Scoffier[15]).

When studying complex alpha spectra with ionization chambers or scintillation spectroscopic equipment, it may be well to bear in mind that distortions of the observed alpha spectra may occur at high source geometry

when coincident conversion electrons or photons can enter the detector and add ionization to that produced by the alpha particle.

If alpha particle energies are to be used to relate nuclear masses or measure nuclear level energies, they must be converted to the Q-values of the process by addition of the recoil energy, an increment equal to the alpha particle energy times the mass ratio of alpha particle and daughter atom. For the most careful rate treatments an additional small energy correction term (cf. eq. 2.2) is added to convert the Q value to the theoretical value for decay of the bare nucleus without any orbital electrons.

A plot for ground transitions of even-even nuclei of the logarithm of the alpha decay half-life vs. decay energy reveals a very smooth behavior except for a break of an order of magnitude at the neutron closed shell of 126. The points for a given element lie on a gently curved line with remarkably little scatter. Nearly straight lines are obtained if the abscissa of the plot is not the energy release Q itself, but the reciprocal square root, $Q^{-\frac{1}{2}}$. (The use of Q_f including electron screening instead of Q is more proper.) Such a plot is shown in fig. 4.1. There is no definite break in the curves to be associated with passage from nuclei of spherical shape into the region of spheroidal shape, which is thought to occur somewhere in the vicinity of 138 neutrons.

If the transitions to excited states of even nuclei or the transitions of odd nuclei are placed on such plots, it is found that they will nearly always lie higher than the lines defined by the ground transitions. A few points will come on or near the lines and may be referred to as "favored" groups. The decay rates to states other than the ground states of even nuclei are often expressed by the "hindrance factor", the ratio by which they depart from the line, or for odd atomic number, from a line interpolated

between even-Z neighbors.

The hindrance factor may be estimated graphically using a plot like fig. 4.1. At the end of this section we give more precise definitions. The rate of a measured group may be compared to semi-empirical rate expressions adjusted to fit the even-even rate data in the regular region beyond the 126-neutron closed shell. One such expression due to Taagepera and Nurmia[16] (cf. eqs. 5.9 and 5.10) gives the theoretical alpha half life as a function of the daughter atomic number Z and the alpha particle energy E_α.

$$\log_{10} t_{\frac{1}{2}\alpha}\,(\text{years}) = 1.61(ZE_\alpha^{-\frac{1}{2}} - Z^{\frac{2}{3}}) - 28.9 \qquad (4.1)$$

An alternative formula below has constants adjusted for separate least squares fitting of the data of several elements[17].

$$\log_{10} t_{\frac{1}{2}}(\text{sec}) = A_Z\, Q_f^{-\frac{1}{2}} + B_Z \qquad (4.2)$$

where Q_f is the effective alpha decay Q value for a bare nucleus ($\approx E_\alpha(\frac{A}{A-4}) + 6.5 \times 10^{-5}\, Z^{\frac{7}{5}}$ MeV). Table 4.2 lists constants that have been given. Alpha emitters below 128 neutrons were not included in obtaining the constants.

Table 4.2

Constants for eq. (4.2)

Z + 2 Parent Atomic Number	A_Z	B_Z
84	129.35	-49.9229
86	137.46	-52.4597
88	139.17	-52.1476
90	144.19	-53.2644
92	147.49	-53.6565
94	146.23	-52.0899
96	152.44	-53.6825
98	152.86	-52.9506

Decay rate data have been treated by Bethe's expression[11] (our eq. 5.24), or similar expressions[18], where the effective nuclear radius is found which satisfies the data.

A treatment of rate data with more fundamental significance, but using formulas simple enough for slide rule or desk calculator, is that of Winslow[17,19]. The derived quantity is called the "surface probability" and is the normalized squared alpha wave amplitude ($r\,\psi_{(r)}$) to be evaluated at some radius in the nuclear surface region.

$$\text{surface probability} = \frac{M\,R\,\ln 2}{\hbar\,k\,t_{\frac{1}{2}\alpha}}\,G_L^2(R) = 0.998\times10^{-22}\sqrt{\frac{A}{A+4}}\;\frac{RG_L^2(R)}{Q_f^{\frac{1}{2}}\,t_{\frac{1}{2}\alpha}\,(\text{sec})} \qquad (4.3)$$

$G_L(R)$ is the irregular Coulomb function, to be evaluated from eq. (5.13), or for L=0 from eqs. (5.12), (5.5), and (5.6). When substitution of numerical values for constants is made, we have

$$\log_{10} G^2(R) = 0.64496\left[\frac{Z\,R\,A}{A+4}\right]^{\frac{1}{2}}\gamma(x) - \tfrac{1}{2}\log_{10}\left(\frac{1-x}{x}\right) \qquad (4.4)$$

with $$x = 0.34726\,Q_f\,R\,Z^{-1}$$

for Q_f in MeV, R in femtometers (10^{-13}cm), Z and A the atomic number and mass number of the daughter nucleus. $\gamma(x)$ is given by eq. (5.6). Values of the surface probabilities have been evaluated at R = 9.3 fm for the heavy region and at R = 8.0 fm for rare earths.

Another fundamental measure of the reduced transition probability is the reduced derivative width δ_L^2 introduced by Thomas[6]. In view of the fact that δ_L^2 definitions differing from the original one have also come into use, it is to be recommended that future analyses express rate data as the reduced width γ_L^2, generally used in nuclear reaction work. It is related to the alpha decay constant λ (= ln 2 / $t_{\frac{1}{2}\alpha}$) as follows:

$$\gamma_L^2 = \frac{\hbar \lambda \, G_L^2 (R)}{2 \, k \, R} \qquad (4.5)$$

where k is the wave number $\left(=0.43757 \left(\frac{A \, Q_f}{A + 4}\right)^{\frac{1}{2}} \times 10^{13} \text{cm}^{-1}\right)$.

Optical model analyses[20] of alpha elastic scattering have shown a sloping attractive nuclear potential subtracting from the Coulombic barrier such that the barrier maximum for S-waves is in the region of 11.0 fm. Clearly it is somewhat unrealistic to extend the unmodified Coulomb functions in to much smaller distances. The WKB barrier penetrability integrals for a diffuse nuclear potential have been evaluated numerically by a computer and tabulated for most known alpha groups[21]. For comparison with shell-model rate theories to be presented in sec. 5, it is desirable to calculate from rate data the widths γ^2 at distances $\lesssim 9$ fm, actually inside the apparent alpha barrier. The expression (5.32) is the WKB expression for γ^2 suitable for computer numerical integration with an optical-model potential. The information on the optical model potential defining the alpha barrier is sufficiently uncertain that for a radius slightly smaller than where the barrier begins we may estimate γ^2 by dividing by 50 the tabulated[21] δ^2 values based on the Igo potential.

In terms of the reduced widths the hindrance factors conforming with general practice are to be calculated as follows:

a) Groups to excited states of even-even nuclei.

The hindrance factor is the ratio of the reduced width γ_o^2 to ground and reduced width γ_{eo}^2 to the excited state. The γ_{eo}^2 value is to be calculated as for an $L = 0$ alpha wave, regardless of the actual L value. (The term "reduced hindrance factor" was proposed for the more fundamental ratio using a γ_{eL}^2 calculated with the Coulomb function for the permitted L value.)

b) Groups in odd nuclei.

There is some variation in usage, but more recent work

involves a ratio, as in (a), where the reference width is an average of the ground widths of the two (or more) nearest even-even neighbors.

5. Decay Rates of Spherical Nuclei

Of primary importance in the rate dependence on energy and nuclear charge is the Coulombic potential barrier. The surface region of the nucleus may be thought of as giving rise to an outward flux of alpha particles, most of which flux is reflected by the barrier to form essentially a standing wave. A tiny fraction penetrates quantum mechanically and appears as a purely outgoing spherical wave at large distance. For problems with spherical symmetry the wave equation through and beyond the barrier region is, of course, separable, allowing us to treat radial solutions of a one-dimensional ordinary differential equation.

Simple decay theory would have the decay constant λ (which equals $\frac{\ln 2}{t_{\frac{1}{2}}}$) given by the product of a penetration factor P and "reduced transition probability" f.

$$\lambda = fP \tag{5.1}$$

Loosely speaking f is the number of collisions per second with the barrier (sometimes f is called the "frequency factor") and P gives the fraction of collisions resulting in transmission.

A first step in the analysis of beta decay rate data is to solve the exterior part of the problem--determining the energy and atomic number dependence arising from density of final states in phase space and values of electron and neutrino wave functions at the nuclear surface. The rate dependence from "external" considerations is expressed in the beta decay f.

value, which when multiplied by the half life constitutes the ft value. The ft value is then a real measure of the "internal" intrinsic rate, being proportional to the reciprocal of the square of the nuclear matrix element. Just so in alpha decay the product of half life and penetration factor P also measures the reciprocal square of a nuclear matrix element for alpha decay. We see thus that the hindrance factor F of alpha decay is quite analogous to the ft value; the "super-allowed" transitions of alpha decay are the ground transitions of the even nuclei, taken as displaying unity hindrance factors. The near-absence of positron emission relative to electron capture for the higher Z nuclei is well-known, and the tiny theoretical f values for positron emission are seen to arise from the small nuclear surface amplitude of the regular solution of the Dirac equation for positrons of modest energy in the repulsive Coulomb field of heavy nuclei. A barrier penetration is involved in high-Z positron emission. There are many treatments of alpha decay with greatly differing formal appearance and similar results, but we shall here reserve our main attention for a treatment bearing great formal resemblance to beta decay theory; this is the treatment originated by Born[22]). In the final theoretical expressions for the alpha decay rate there is a direct proportionality to the square of an alpha wave amplitude at the nuclear surface, namely the regular solution of the alpha wave equation in the region beyond the nuclear surface. Examination of these solutions (regular Coulomb functions) will immediately give the answer to the external part of the problem.

For the zero-angular-momentum (S-wave) problem the wave function $\psi(r,\theta,\phi)$ of the alpha (with respect to the center of the daughter nucleus) is independent of angle. The function $u(r) = r\psi(r)$ must satisfy the one-dimensional wave equation

$$-\frac{\hbar^2}{2m}\frac{d^2u}{dr^2} + [V(r)-Q_f]u = 0 \qquad (5.2)$$

where $\underline{m}$ is the reduced mass = $\left(\frac{m_\alpha m_d}{m_\alpha+m_d}\right)$ and $\underline{Q_f}$ is the total energy release for a bare nucleus.

The simplest barrier approximation is to assume a pure Coulombic potential beyond up to a radius $\underline{R_o}$, somewhere in the outer fringe region of the nucleus.

$$V(r) = \frac{2Ze^2}{r} \quad , r > R_o \qquad (5.3)$$

where $\underline{Z}$ is the atomic number of the daughter and $\underline{e}$ is the elemental charge in esu. We seek the solution that is exponentially increasing through the barrier region $\left(r < \frac{2Ze^2}{Q_f}\right)$ and goes over to an oscillatory solution at greater distances with an oscillation amplitude tending to unity at very great distance.

Solutions of the WKB type are quite good everywhere except in the immediate vicinity of the classical turning point $R_t = \frac{2Ze^2}{Q_f}$, and there are connection formulas for joining the solutions in the regions inside and outside the barrier. The regular solution is as follows:

$$F(r,Z,Q_f) = \frac{k^{\frac{1}{2}}}{2\,q^{\frac{1}{2}}} \exp\left[-\int_r^{R_t} q(r_1)dr_1\right] \qquad (5.4)$$

with $q(r) = \frac{1}{\hbar}\left[2m\left(\frac{2Ze^2}{r} - Q_f\right)\right]^{\frac{1}{2}}$

Bethe introduced[11]) a convenient parametrization for the analytical expression of the integral of eq. (5.4). He defined a dimensionless parameter $\underline{x}$ defined as the ratio of the energy Q_f to the Coulombic potential at the inner barrier radius. He also defined a function $\underline{g}$ independent of Q_f.

$$g = \frac{2e}{\hbar} (mZr)^{\frac{1}{2}} \qquad (5.5)$$

The integral in the exponent of eq. (5.4) is equal to the product of g and a function $\gamma(x)$.

$$\gamma(x) = \tfrac{1}{2}\pi x^{-\frac{1}{2}} - x^{-\frac{1}{2}} \text{ arc sin } (x^{\frac{1}{2}}) - (1-x)^{\frac{1}{2}} \qquad (5.6)$$

The function $\gamma(x)$ is singular at x=0, approaching a limiting behavior of

$$\lim_{x \to 0} \gamma(x) = \tfrac{1}{2}\pi x^{-\frac{1}{2}} - 2 \qquad (5.7)$$

Bethe has given a graph[11]) of the function $\gamma(x)$, but for careful calculations in alpha decay applications greater accuracy is often needed. Tables of the arc sin can be used with eq. (5.6) for more accurate work. The part of function $\gamma(x)$ remaining after subtraction of the singular function of eq. (5.7) can be expanded about some $\underline{x}_o$ value, preferably in the vicinity of values to be used. A Taylor series expansion about $\underline{x}_o$ of $\frac{1}{4}$ takes a simple form and centers within the region of alpha decay $\underline{x}$ values.

$$\gamma(x) = \tfrac{1}{2}\pi x^{-\frac{1}{2}} - \frac{1}{3}\pi - \frac{\sqrt{3}}{2} + \frac{\sqrt{6}}{2}\left(x - \tfrac{1}{4}\right) + \ldots \qquad (5.8)$$

If one drops the last term of eq. (5.8), uses eq. (5.5), and then considers that the basic rate equation is a constant times the exponential part of eq. (5.6) squared, one gets the expression used by Taagepera and Nurmia in correlating rate data[16]). They have eliminated any explicit dependence on the radius $\underline{R}_o$ in their second term by considering approximately that $\underline{R}_o \approx 2.04\, Z^{\frac{1}{3}}$

$$\lambda = C_o \exp\left[-\frac{2\pi\, 2^{\frac{1}{2}} e^2 m^{\frac{1}{2}}}{\hbar} \frac{Z}{Q_f^{\frac{1}{2}}} + \frac{8.47\, e\, m^{\frac{1}{2}} (2.04)^{\frac{1}{2}}}{\hbar} Z^{\frac{2}{3}}\right] \qquad (5.9)$$

where we have changed their coefficient 8 in the second term to 8.47, to correspond with our expansion about $\underline{x}_o = \frac{1}{4}$ rather than the usual $\underline{x}_o = 0$.

Converting to a form practical for approximate calculation of alpha decay rates of even nuclei, they give the form

$$\log_{10} t_{\frac{1}{2}} = C_1(ZQ_f^{-\frac{1}{2}} - C_3 Z^{\frac{2}{3}}) - C_2 \qquad (5.10)$$

with $C_1 = 1.70\ (\text{MeV})^{\frac{1}{2}}$

$C_3 = 1.13\ (\text{MeV})^{-\frac{1}{2}}$ being our theoretical values.

The R_o values from their expression are about those needed by the one-body models of alpha decay in which the alpha particle initially is considered confined in the lowest state in a flat potential well with walls at R_o. From Bethe's one-body model[11], they get $C_2 = 28.0$ for $t_{\frac{1}{2}}$ in years. They then set C_3 to unity, use the alpha particle energy instead of Q_f, and determine empirical values C_1' and C_2' that fit especially the data of Rn^{215}, Ra^{226}, U^{236}, and Th^{232}, namely $C_1' = 1.61$ and $C_2' = 28.9$.

Many analyses of rate data have been made in earlier times, where one assumes the "one-body" model, or some other model, to give the pre-exponential factor in an equation like eq. (5.1), with $F^2(R_o, Z, Q_f)$ of eq. (5.4) substituted for P. The parameter R_o is adjusted for each nucleus to give agreement[23]. Such calculated "effective radii for alpha decay" are one way of displaying reduced transition probabilities for systematic studies, but results of shell-model alpha-decay calculations in recent times show some pronounced dependence of reduced transition probabilities on the particular shell model configurations, especially around 126 neutrons. Thus, it would be a mistake to associate fluctuations in the calculated R_o values with actual changes in the mean square radius of the nuclear matter density distribution. The early analyses of alpha rate data to yield R_o values were of great importance in providing nuclear physics with some of the first good estimates of nuclear sizes[5]. These estimates have been superseded by other

experimental measurements, giving radius values in less model-dependent and more accurate ways. For the nuclear charge distribution high energy electron scattering has played the essential role with mu-mesic X-ray energies supplying supplemental information[24]). The small rms radii from scattering were at first surprising in that they were so much smaller than the alpha decay and nuclear reaction cross section radius values. New degrees of sophistication on questions of nuclear sizes were required--firstly, the notion of a diffuse edge in nuclear density distributions and nuclear potentials, and secondly, the notion that nuclear reaction potentials extend generally to larger radii than the matter distribution. Our present best information about the effective nuclear potential for alpha particles in alpha decay comes from optical model analyses of alpha elastic differential scattering cross sections. The optical potentials come from experiments with more energetic alpha radiation than occurs in alpha decay, and the energy dependence of the potentials has not been well studied. The optical potentials give considerably weaker barriers than required by the one-body models of alpha decay.

With these reservations in mind, let us develop a treatment of the one-body model preliminary to consideration of the modern shell-model alpha theory.

First we should summarize the notation and review a few properties of the standard Coulomb functions. By substitution and rearrangement of the radial wave equation (5.2), generalized to include $L > 0$ and with the Coulombic potential of eq. (5.3) extending over all space, we get the form

$$\frac{d^2u}{d\rho^2} + \left[1 - \frac{2\eta}{\rho} - \frac{L(L+1)}{\rho^2}\right] u = 0 \qquad (5.11)$$

where $\rho = \underline{k}r$ and $\eta = \frac{2Ze^2m}{\hbar^2 k} = 0.6300 \frac{Z}{\sqrt{Q_f}} \sqrt{\frac{A}{A+4}}$ with $\underline{k}$, the wave number

$$\left(= \frac{(2mQ_f)^{\frac{1}{2}}}{\hbar} = 0.4376\sqrt{\frac{AQ_f}{A+4}} \cdot 10^{13}\,\mathrm{cm}^{-1} \right) .$$

The two linearly independent solutions are designated $F_L(\rho,\eta)$, regular at the potential singularity at the origin, and $G_L(\rho,\eta)$, irregular at the origin. The functions go over at large distance to sine and cosine functions, respectively, with argument $[\rho - \eta \ln 2\rho - \frac{L\pi}{2} + \arg\Gamma\,(i\eta+L+1)]$.

For $F_o(\rho,\eta)$ we may as well use eqs. (5.4) through (5.6), since the Bethe parametrization[11], where the g parameter is independent of energy, is often more convenient than the standard Coulomb parametrization. Also we give $\underline{G_o}$ in the earlier notation of eq. (5.4).

$$G_o(r,Z,Q) = \frac{k^{\frac{1}{2}}}{q^{\frac{1}{2}}} \exp\left[\int_r^{R_t} q(r_1)dr_1\right] \tag{5.12}$$

Fröberg[25] gives the Ricatti approximation formulas for these functions out to many terms. A WKB expression for all $\underline{L}$ is

$$G_L(\rho,\eta) = \kappa^{-\frac{1}{2}} (\eta^2 + \ell^2)^{-\frac{\ell}{2}} \left(\ell\kappa + \frac{\ell^2}{\rho} + \eta\right)^{\ell} \exp\left[\pi\eta - \eta \arccos \frac{\eta+\rho}{\sqrt{\eta^2+\ell^2}} - \rho\kappa\right] \tag{5.13}$$

with $\kappa = +\left[\frac{2\eta}{\rho} + \frac{\ell^2}{\rho^2} - 1\right]^{\frac{1}{2}}$.

The ordinary WKB form substitutes $(L(L+1))^{\frac{1}{2}}$ for ℓ, but the preferred Langer modification substitutes $L + \frac{1}{2}$ for ℓ.

Our starting point for developing shell model alpha decay theory will be the basic quantum mechanical perturbation rate expression

$$\lambda = \frac{2\pi}{\hbar} |H_{if}|^2 \frac{dn}{dE} \tag{5.14}$$

where $\underline{H_{if}}$ is the transition perturbation matrix element on $\frac{dn}{dE}$ is the density

of final states. We will first develop the theory for S-state decay by the one body-model, where the nuclear model consists merely of an alpha particle in its lowest quasi-stationary state in a potential well. This method of formulation will be seen to have a close parallel to treatments by Born[22], Casimir[26], and Mang[27].

Figure 5.1 illustrates the potentials assumed for the initial and for the final states, and the perturbation Hamiltonian for the transition is the difference of these potentials beyond the radius where the two potentials agree.

$$H_{if} = \int_{R_o}^{\infty} u_f^* (V_i - V_f) u_i \, dr = 2Ze^2 \int_{R_o}^{\infty} \left(\frac{1}{R_o} - \frac{1}{r}\right) u_f^* u_i \, dr \qquad (5.15)$$

The wave function u_i is simply a finite square-well solution, normalized to probability of one.

$$u_i(r) = \begin{cases} \simeq \sqrt{\frac{2}{R_o}} \sin k_i r & , \; r \leqslant R_o \\ = B\sqrt{\frac{2}{R_o}} \, e^{-\frac{\sqrt{2m\left(\frac{2Ze^2}{r} - E\right)}}{\hbar}} & , \; r \geqslant R_o \end{cases} \qquad (5.16)$$

with B determined by matching inner and outer solutions at R_o. The final-state wave function, which need be defined only beyond R_o, where the perturbation energy first takes on a non-zero value, is to be the regular Coulomb solution $F_o(kr)$, normalized to unity within a large box, the outer wall of which is adjusted to a node a distance L away with $L \gg R_o$.

$$u_f = \sqrt{\frac{2}{L}} \, F_o(kr) \qquad , \; r \geqslant R_o$$

From the energy equation for states of n nodes in a square well of length L we can evaluate the density of final states needed for eq. (5.11).

$$E_n = \frac{\pi^2 \hbar^2 n^2}{2 m L^2}$$

$$\frac{dn}{dE} = \frac{m L}{\pi \hbar^2 k} \tag{5.18}$$

where m is the reduced mass, and k is the wave number at very large r.

To evaluate the matrix element simply we will make use of the fact that the initial and final wave functions are solutions of the wave equation in their respective potentials.

$$\frac{2Ze^2}{R_o} u_i = E u_i + \frac{\hbar^2}{2m} \frac{d^2 u_i}{dr^2} \tag{5.19}$$

and a similar equation for u_f but with R_o replaced by r. Thus, substituting into eq. (5.15)

$$H_{if} = \frac{\hbar^2}{2m} \int_{R_o}^{L} \left(u_f^* \frac{d^2 u_i}{dr^2} - \frac{d^2 u_f^*}{dr^2} u_i \right) dr$$

$$= \frac{\hbar^2}{2m} u_f^* \frac{d u_i}{dr} \left(1 - \frac{1}{u_f^*} \frac{d u_f^*}{dr} \cdot \frac{u_i}{\left(\frac{du_i}{dr}\right)} \right) \Bigg|_{R_o}^{L} \tag{5.20}$$

The contribution at the upper limit is seen to go to zero by the vanishing of u_i at large r. The replacement of the radial integration by a function evaluated at R_o is the one-body equivalent of Mang's replacement[27]) of a volume integral by a surface integral at R_o. A further simplification has been noted by Mang; if the potentials V_1 and V_2 are equal at R_o, the logarithmic derivatives of u_i and u_f at R_o are equal in magnitude and opposite in sign, so the two terms of eq. (5.20) make equal contributions. Hence,

$$H_{if} = - \frac{\hbar^2}{m} u_f^* \frac{d u_i}{dr} \Bigg|_{r=R_o} \tag{5.21}$$

Substituting eqs. (5.21) and (5.18) into eq. (5.14) we get the result

$$\lambda = \frac{2}{\hbar\, k\, R_o} \cdot \frac{\hbar^2 R_o}{2m} \left| \frac{d\, u_i}{dr} \right|^2_{r=R_o} \cdot 4 \left| F_o \right|^2 \qquad (5.22)$$

We wish to rearrange the solution so as to identify and extract the expression for the reduced derivative width introduced by R. G. Thomas by the defining equation[6])

$$\lambda_L = \frac{2\,\delta_L^2}{k R_o \hbar} \frac{F_L^2 + G_L^2}{(F_L F_L' + G_L G_L')^2}\Bigg|_{\rho=kR_o} \approx \frac{2\,\delta_L^2}{k\, R_o\, \hbar\, (G_L')^2_{\rho=kR_o}} \approx \frac{2\, k\, R_o \gamma_L^2}{\hbar\, G_L^2} \qquad (5.23)$$

where the prime denotes differentiation with respect to ρ.

From first order WKB approximation we have that G'F within the barrier is nearly equal to $\frac{1}{2}$. Thus, from our theory,

$$\delta_o^2 = \frac{\hbar^2 R_o}{2m} \left| \frac{d\, u_i}{dr} \right|^2_{r=R_o} .$$

This result agrees with the one-body expression from Thomas' R-matrix theory (see eq. (24.5) of ref. 6). From the expression (5.15), with substitution for k_i of the lowest allowed value within a square well of length R_o, we determine the square of the derivative explicitly as $\frac{2\pi^2}{R_o^3}$. Thus, from eq. (5.22) and the WKB approximation for $F_o(kR_o)$ the following expression results:

$$\lambda = \frac{2^{\frac{1}{2}} \pi^2 \hbar^2}{m^{\frac{1}{2}} R_o^3 (B_c - E)^{\frac{1}{2}}}\, e^{-2g\gamma(x_o)} \qquad (5.24)$$

where $B_c = \frac{2Ze^2}{R_o}$. This result is identical to Bethe's one-body model expression[11]). With a few approximations the lowest (nodeless) solution of Preston's simultaneous equations again gives the same result[28,29]).

Our treatment of alpha decay above would be even closer to Mang's if we used delta-function normalization of our u_f rather than normalization in a box with periodic boundary conditions.

$$\int_0^\infty u_f^*(r,E)\, u_f(r,E')dr = \delta(E-E')$$

With this form of normalization the $\frac{dn}{dE}$ factor of eq. (5.14) is replaced by unity. Henceforth, we shall in fact use this normalization and shall distinguish the matrix elements so determined by primes. The primed matrix element H'_{if} has the dimensions of the square root of energy.

Let us now consider a simple problem that will be illustrative of the principles involved in Mang's shell-model theory of alpha decay. This problem considers two spin-less nucleons in a one-dimensional harmonic oscillator well. It is equivalent to visualize this problem as the barrier penetration problem of one particle in a two-dimensional harmonic oscillator potential, as schematically indicated in the contour diagram of fig. 5.2. There exist saddle points leading to valleys only along the line $x_1=x_2$, and the valleys may be reached by tunnelling through the Coulombic barrier, as indicated in the potential profile along $x_1=x_2$ (fig. 5.2). We assume that a section across the valley always gives a parabolic potential of constant width, hence a Gaussian wave function of internal motion of the quasi-deuteron at large distance.

How is one to evaluate the matrix element now? It is only necessary to generalize eq. (5.21) for the multi-particle, multi-dimensional problem by specifying that there be additionally an integration over all co-ordinates normal to the coordinate specifying the cluster's center-of-mass motion along the channel valley, evaluated at R_o.

For this simple example it is easy to write a shell-model-like product of two harmonic oscillator wave functions in x_1 and x_2. One then transforms to center of mass $\left(\frac{x_1+x_2}{2}\right)$ and relative (x_1-x_2) coordinates and easily integrates over the relative coordinate. The matrix element so obtained bears

a resemblance to the following expressions applicable to the full four-particle, three-dimensional problem[27]).

$$H'_{if} = -\frac{\hbar^2}{m}\,\phi^*_L(R_o)\int d\xi_\alpha\, d\xi_k\, R_o^2\, d\Omega\, \chi^*_\alpha(\xi_\alpha)\sum_{m_f}(L\ I_f\ m_i - m_f m_f \mid I_i m_i)Y^*_{L\ m_i-m_f}(\theta,\phi)$$

$$\Psi^*_{I_f\ m_f}\,\sigma(\xi_k)\,\frac{d}{dr}\,\Phi_o\,I_i m_i\,(\text{space-spin coordinates of A+4 nucleons})\Big|_{r=R_o} \qquad (5.25)$$

where $\underline{M}$ is the alpha reduced mass. The quantity $\chi_\alpha(\xi_\alpha)$ is the internal wave function for the alpha particle; it involves nine relative position coordinates and four spin coordinates, designated as ξ_α. The function $\Psi(\xi_k)$ is the shell-model wave function for the daughter nucleus, involving space and spin coordinates ξ_k of $\underline{A}$ nucleons. The position coordinates of the alpha center-of-mass are $\underline{r}$, θ and ϕ, and Φ_o is the initial parent wave function. There is a Clebsh-Gordan summation over angular momentum projections in the final state, thus insuring that there is conservation of total angular momentum. The function $\phi_L(R_o)$ is the regular solution of the radial equation for the alpha in the external potential (not necessarily pure Coulombic) beyond $\underline{R_o}$, with energy delta function normalization. For a Coulomb potential we have

$$\phi(R_o) = \left(\frac{2m}{\pi\hbar^2 k}\right)^{\frac{1}{2}} \quad \frac{F_o(kR_o)}{R_o}$$

It is better for using realistic numerical shell-model radial wave functions to cast eq. (5.25) into an equivalent form not involving a radial derivative of the initial function. We see by going back to eq. (5.20) that it is equivalent to throw the derivative onto the final wave function giving eq. (5.21) the new form

$$H'_{if} = \frac{\hbar^2}{m}\,u_i\,\frac{du^*_f}{dr}\Big|_{r=R_o}$$

and eq. (5.25) is similarly modified by a sign change and movement of the radial derivative from the function Φ over to ϕ_L^*.

Mang's procedure[27] for evaluating the matrix element of eq. (5.25) is as follows: the parent wave function Φ_o is to be expanded using fractional parentage coefficients (or their second-quantization equivalents) into products of functions of two protons and two neutrons times a core function of the remaining A nucleons. The integration over $d\xi_k$ projects out one (or if there is configuration mixture in the daughter state, more than one) term having the same "core function" as the daughter wave function. The remaining function of two protons and two neutrons must be re-expressed or expanded (at least near R_o) in terms of functions of the relative-motion coordinates ξ_α and the center-of-mass coordinates. Then the integrations may all be carried out.

This procedure is not as formidable as it appears, for Mang is able to effect considerable simplification, using special properties of harmonic oscillator wave functions, allowing expansion of the shell-model product functions of nucleon coordinates into harmonic oscillator functions of the relative and center-of-mass coordinates. After the integration over $d\xi_\alpha$ he is able to collect the resulting series of terms into Laguerre polynomials.

We note at this point that Mang's definition (his eq. I.20 of ref. 30) of the reduced width δ^2 differs from the original one of Thomas[6] by about a factor of six.

$$\delta^2_{\text{Thomas}} = \delta^2_{\text{Mang}} \cdot \frac{R_o q_L(R_o)}{2} \qquad (5.26)$$

where q_L is as defined by eq. (5.4). The change does not affect the practical applications that have been made [30,31], since it is relative transition probabilities that are compared with experiment. Mang made his particular definition to facilitate comparison with δ^2 values tabulated by Rasmussen for

barrier penetrabilities with a sloping nuclear potential[21]). Rasmussen's δ^2 values are somewhat differently defined from those of either Thomas or Mang, and this matter is discussed further in a later section. The confusion over δ^2 definitions does not alter the essential results of shell model theory, which claims only good relative decay calculations in its present form.

Since there has been a little confusion in definition of the reduced derivative width δ_L^2 originated by Thomas, it would seem desirable henceforth to express alpha decay rate information in terms of the ordinary reduced width γ_L^2 commonly used in nuclear reactions. The δ^2 value had a special usefulness for comparison with one-body theory, but γ^2 is as convenient for many-body theory.

The reduced width is related to the matrix element H'_{if} in the following way:

$$\gamma_L = \left(\frac{\pi}{\rho_o}\right)^{\frac{1}{2}} G_L(\eta,\rho_o) H'_{if} \qquad (5.27)$$

where ρ_o and $G_L(\eta,\rho_o)$ are the values of $\underline{kr}$ and of the irregular Coulomb function at the connection distance $\underline{R_o}$.

Simpler formulas than Mang's have been derived by evaluation of eq. (5.25) in the limit of a delta-function alpha particle[32,33]). Comparisons against the more sophisticated finite alpha calculations suggest that the simple formulas can be quite good for relative decay rate calculations when a correction factor is introduced[12]).

We summarize here some expressions for relative values of γ_α^2 from the delta-function approximation (cf. ref. 12):

Spherical even-even (to or from closed shells or subshells) (Favored Decay)

$$(j_n)_o^{\pm 2}\ (j_p)_o^{\pm 2}\ \text{core} \rightleftarrows \text{core}$$

or

$$(j_n)_o^{\pm 2}\text{core} \rightleftarrows (j_p)_o^{\pm 2}\text{core} \qquad (5.28)$$

$$\gamma_o = \text{const.}\ (2j_n + 1)^{\frac{1}{2}}\ R_n^2 \cdot (2j_p + 1)^{\frac{1}{2}}\ R_p^2\ B_n\ B_p$$

The quantities R_n, R_p, etc. are the values of the nucleon radial wave functions, evaluated at the chosen connection radius R_o. The constant depends on the alpha size and nuclear size and has been given in ref. 33, but the formulas are only reliable for relative transition probabilities.

The delta-function model tends to overestimate the contributions of high-j orbitals. An approximate correction factor $B_n = \exp[-0.013\ \ell_n(\ell_n + 1)]$ brings the above formula into good agreement with the finite-sized-alpha formulas. B_p is of like form. For decay not at closed shells the expressions are to be multiplied by appropriate fractional parentage coefficients. The contribution of components with non-zero seniority in decay from or to excited states is as follows:

$$\left\{(j_n)^1,\ (j_n')^1\right\}_L\ (j_p)_o^2 \rightleftarrows \text{core}$$

$$\gamma_L = \text{const.}(2j_p + 1)^{\frac{1}{2}}[(2\ell_n + 1)^{\frac{1}{2}}\ (2\ell_n' + 1)^{\frac{1}{2}}(\ell_n\ \ell_n'\ 00|L0)\ W(\ell_n\ j_n\ \ell_n'\ j_n';\ \tfrac{1}{2}L)]$$

$$\cdot\ R_p^2 \cdot R_n\ R_n'\ B_p\ B_n'$$

where for the cases allowed by alpha decay selection rules the whole quantity in brackets can be greatly simplified[12])

$$\gamma_L = \text{const.}(-)^{\ell_n}(2j_p + 1)^{\frac{1}{2}}\ (2j_n + 1)^{\frac{1}{2}}\ (L\ j_n\ 0 - \tfrac{1}{2}|j_n'\ -\tfrac{1}{2})R_p^2\ R_n\ R_n'\ B_p\ B_n'$$

$$= \text{const.}(-)^{\ell_n + j_n - \frac{1}{2}} \left[\frac{(2j_p+1)(2j_n+1)(2j_n'+1)}{2L+1} \right]^{\frac{1}{2}} (j_n' \; j_n \; \tfrac{1}{2} \; -\tfrac{1}{2} \mid L0)$$

$$R_p^2 \, R_n \, R_n' \, B_p \, B_n' \qquad (5.29)$$

Equation (5.29) clearly reduces to eq. (5.28) for L=0 and $j_n' = j_n$. The correction factor B_n' is a function of the relative momentum and may be written $B_n' = \exp\left\{ \frac{-0.013}{2} \left[\ell_n(\ell_n+1) + \ell_n'(\ell_n'+1) - \frac{L(L+1)}{2} \right] \right\}$. For $\underline{R(r)}$ values we may use three-dimensional harmonic oscillator functions[33]), or better, use the numerical wave functions of Blomqvist and Wahlborn[34]), calculated for a diffuse potential well at Pb^{208}. Table 5.1 gives their radial functions at radial distances of 8 fm and 9 fm, typical distances used as connection radii in the literature. The tabulated values are 1000 times the normalized values, where the distances are in fermis. They are to be divided by $\underline{r}$ to give our $\underline{R(r)}$ functions for eq. (5.28).

Table 5.1

Radial Nucleon Wave Functions of Blomqvist and Wahlborn

r	Protons					Neutrons						
	$1i_{13/2}$	$2f_{7/2}$	$1h_{9/2}$	$3s_{1/2}$	$2d_{3/2}$	$1i_{11/2}$	$2g_{9/2}$	$^3P_{1/2}$	$2f_{5/2}$	$^3P_{3/2}$	$1i_{13/2}$	$d_{5/2}$
8 fm	316	361	195	304	252	289	461	428	369	432	347	454
9 fm	127	172	74	136	104	142	299	272	202	272	159	392

The effect of configuration mixing on alpha decay rates is profound, as calculations of Harada[35]), Mang and Rasmussen[36]), and Soloviev[37]) have shown. The mixing smooths and averages out the rapid rate fluctuations from nucleus to nucleus that are otherwise predicted. Furthermore, the configuration mixing of the type induced by attractive residual forces produces a large over-all enhancement in the theoretical decay rates.

Zeh[37] tabulates absolute δ^2 values with Mang theory for several choices of parameters for the ground transition in Po^{211}. Multiplying his values by the correction factor of about 6, according to our eq. (5.26), his δ^2 values range from $8.4 \cdot 10^{-7}$ MeV for R_o of 9 fm to $3.6 \cdot 10^{-4}$ MeV for R_o of 7.5 fm. Using again the optical-model barrier penetrability these calculations represent theoretical decay rates smaller than experimental by factors from $2 \cdot 10^4$ to 5.

When we see this sort of drastic variation with R_o, it is evident that the present form of shell-model alpha theory does not yield very meaningful absolute rate calculations. Wilkinson[38] has questioned the theory, taking shell-model calculations by Harada[35] to show that shell-model theory gives values too low by factors of 10^2 to 10^4, depending on the detailed assumptions made. The conclusions are critically dependent on the barrier thickness, and it is thus appropriate that we examine the basis for the optical model potential used to define the barrier in recent discussions of the absolute rate theory.

Various alpha particle reaction cross sections yield some information on how far the nuclear potential for alpha particles extends. Rather large radii are generally indicated[5]. It is alpha elastic scattering differential cross sections, mostly at 40 MeV, that have provided the best information on range and diffuseness of the nuclear potential for alpha particles. It is an appealing idea to try to derive reduced transition probabilities without the introduction of an arbitrary nuclear radius R_o or of arbitrary assumptions about potentials. With such motivation Rasmussen carried through numerical analysis[21] of experimental energy and rate data using the real part of the optical model potential derived by Igo[20] from scattering data.

Igo's potential is

$$V_n(r) = - 1100 \exp\left(\frac{1.17A^{1/3}-r}{0.574}\right) \text{MeV}$$

with his qualification that the formula is valid only for the potential less than about 10 MeV. By using the formula somewhat beyond this expressed validity range we can define a potential barrier for alpha decay beginning at the inner turning point given by Coulombic plus nuclear potential. (We must regard this potential as uncertain for our barrier purposes. Not only are alpha decay energies far below the scattering experimental energies but the Woods-Saxon potentials used to fit scattering data and on which Igo's exponential potential is based give thicker barriers for alpha decay.) The simple WKB barrier integral was evaluated by a computer for all known alpha groups, and the tabulation of the penetrability exponentials is a useful reference for making theoretical comparisons. We note again (cf. sec. 4) that this work introduces a definition of δ^2, the reduced derivative width, which differs from the original definition of Thomas[6]). The exponential penetrabilities tabulated by Rasmussen[21]) should very closely represent the fraction of incident probability current transmitted through the barrier, but the reduced width γ^2 (or δ^2) depends not only on probability current, but also on the characteristic kinetic energy of the alpha at the arbitrarily specified R_o. If R_o is chosen within the barrier region, the γ^2 (or δ^2) calculated from data is very sensitive to the value of R_o. Also, as is apparent from the preceding discussion on absolute rate calculations from shell-model theory, this theory does not seem presently capable of giving reasonable theoretical reduced widths as far out as the barrier region.

From the standpoint of validity of WKB wave functions, R_o is best chosen not too close to the inner turning point, R_i, of the diffuse barrier.

The connection distance R_o may be chosen far enough out that the attractive nuclear potential can be neglected compared to the Coulombic. Then one can use eq. (5.23) and eqs. (5.13), or (5.12), (5.5), and (5.6) to relate the experimental decay rate to the reduced width γ^2.

$$\gamma_L^2 = \frac{\hbar\lambda_L}{2\,k\,R_o} \quad G_L^2(R_o) \tag{5.30}$$

The use of this equation with G_L the irregular Coulomb function would correspond to the usual alpha decay rate analysis, but the large R_o places a severe strain on shell-model theory for alpha width.

It is also possible to use a connection distance R_o closer in. If it is chosen close to the inner turning point of the barrier, some numerical continuation of the irregular Coulomb functions needs to be made for substitution into eq. (5.30). If R_o is chosen sufficiently smaller than the inner turning point for the first-order WKB approximation to be valid, then with WKB connection formulas we can write the expression for the irregular function suitable for substitution into eq. (6.4).

$$G_L(R_o) = \frac{2k^{\frac{1}{2}}}{k(R_o)^{\frac{1}{2}}} \cos\left(\int_{R_o}^{R_i} k(r)\,dr - \frac{\pi}{4}\right) \exp\left(\int_{R_i}^{R_t} q_L(r)dr\right) \tag{5.31}$$

where the G_L function is now not a Coulomb function but the continuation of the irregular Coulomb function into the classically allowed region inside the inner turning point. Substituting eq. (5.31) into eq. (5.30) we have an equation suitable for calculation of γ^2 from data.

$$\gamma_L^2 = \frac{\lambda\hbar}{R_o k(R_o)}\, 2\cos^2\left(\int_{R_o}^{R_i} k(r)dr - \frac{\pi}{4}\right) \exp\left(2\int_{R_i}^{R_t} q_L(r)dr\right) \tag{5.32}$$

Since this definition is in accord with nuclear reaction usage, this expression is a better one to be applied to rate data than the following expression

independent of R_o and the potential inside the turning point, which Rasmussen used[21]):

$$\delta^2 = 2\pi\hbar\lambda \exp\,(2 \int \text{barrier})$$

With eq. (5.32) we see it is clearly impossible to avoid specification of an arbitrary R_o and of the potential everywhere beyond R_o if one would calculate γ_L^2 from rate data. However, the choice of R_o in the classically allowed region not too far from the barrier can yield γ^2 values much less sensitive to choice of R_o than a choice within the barrier.

We note that we can use the calculated δ^2 values of Rasmussen subject to some qualification. If we are fairly close to the barrier onset ($\approx$ 9.3 fm) or if we assume the nuclear potential to level off inside the inner turning point so that the integral in the argument of the cosine function in eq. (5.31) is small, then the factor $2\cos^2(\int kdr - \frac{\pi}{4})$ may be approximately replaced by unity. Experimental γ^2 values may be obtained by dividing the tabulated δ^2 values by $2\pi R_o k(R_o)$. We must specify a kinetic energy, hence $k(R_o)$, at R_o. If the kinetic energy at R_o were as high as ~ 25 MeV the tabulated δ^2 values are to be divided by ~ 100 to get γ^2, if the energy were ~ 6 MeV at R_o, the division is by ~ 50.

Figure 6.1 from ref. 21a graphs the δ^2 values calculated from data for ground transitions of even nuclei.

We see now the uncertainties associated with testing of absolute rate theory, but there are clearly unanswered questions regarding absolute rates and shell-model rate theory.

To gain some for the insight into the problem of absolute rate theory let us go back to the basic assumptions of the shell-model alpha theory, as can be visualized from fig. 5.1. If we had regions of overlapping validity of our internal Hamiltonian (for the initial state) and our external

Hamiltonian, it would not matter where within the region of simultaneous validity that we chose R_o; the answer would be the same. The perturbation energy integrand takes on non-zero values only beyond the distance where the internal Hamiltonian begins to be in error. We agree with Wilkinson[38]) that the pure shell-model wave function fails badly in representing the amount of nucleon clustering in the vicinity of 9 fermis, the tail of the matter distribution, but it may, with addition of some configuration mixture, fairly well represent the alpha clustering at distances less than ~ 8 fm.

The addition of reasonable amounts of configuration mixture in the wave functions results in an order of magnitude increase for the even polonium isotopes. Harada[35]) obtained factors of 10 for Po^{210} and 5 for Po^{212}, and Zeh[37]) finds an enhancement of 12 for Po^{210} using a pairing-force wave function. The pairing-force model treats neutrons and protons completely independently, hence is not capable of representing n-p clustering tendencies. The approximation for most purposes is rather good for heavy nuclei, where neutrons and protons are filling orbitals in different major shells. To exploit the attractive n-p force, the ordinary pairing-force wave function must necessarily break pairs at the cost of pairing energy of like nucleons. Calculations for Po^{212} indicate less than an order of magnitude additional enhancement arising from mixing due to n-p forces[33]).

As we add configuration mixture in the shell-model representation, we can, in principle, extend the validity of the initial state wave function as far out as we please and represent whatever amount of clustering occurs. Actually it becomes impractical in the shell model to mix configurations beyond the adjacent major shells, such as would be necessary to describe clustering in the surface.

Thus, it may not be practicable to extend the region of validity of the inner wave function by configuration mixture as far out as the barrier

region. What, then, can be done to the final wave function to bring its region of validity in closer? The answer is similar to that concerning improvement of the inner wave function. A one-term product wave function of daughter internal ground state function, alpha ground state internal function, and the wave function of the alpha position coordinates is only a first approximation. A many-term final wave function including excited states of the daughter nucleus can bring the external region of validity inward. We can learn from nuclear reactions which excited states are most important to include in the description. Probably of most importance are those states strongly excited by inelastic scattering of alpha particles; these states are usually characterized by having strong, collectively-enhanced, electric multipole matrix elements connecting them to ground. Where we are dealing with daughter nuclei which have states strongly excited by Coulomb excitation, we may need to include such states in the alpha decay wave function even at distances well out into the barrier and away from short-ranged nuclear forces. In thus contemplating the direction from which future improvements in alpha rate theory may come, we are led to consider the work on alpha wave propagation through the anisotropic barrier of spheroidal nuclei. The work is necessary to any fundamental analysis of decay of spheroidal nuclei, and it is also of interest as an example of the manner in which future theoretical work could bring into the description more of the inelastic scattering states.

6. Decay Rate Theory Including Non-Central Interactions

The work of M. A. Preston first treated carefully the barrier effects of coupling between the alpha particle and the internal degrees of freedom via the electromagnetic radiation field[39]). He showed that in the presence of non-central fields the alpha wave function is to be found as a solution of a set of coupled radial differential equations. Other later work took more careful account of conservation of angular momentum[40]) and established quantitative relations between coupling terms in the equations and measurable nuclear parameters such as electromagnetic reduced transition probabilities $B(E\lambda)$ (or the derived intrinsic quadrupole moment Q_o)[17]).

Let us consider the extension of ground alpha decay of even nuclei by inclusion of the first excited state of the daughter (usually 2+). The final-state wave function appropriate for our earlier matrix element formulas of sec. 5 will now be expressed as

$$\Psi_f = \frac{\chi_o}{r}\left[u_o(r)\,\psi_{oo}(x_i)\,Y_{oo}(\theta,\phi) + u_2(r)\sum_m (22\text{-}mm\,|\,00)\,\psi_{2\text{-}m}\,Y_{2m}(\theta,\phi)\right] \tag{6.1}$$

where the $\psi_{Im}(\chi_i)$ are the wave functions of the daughter nucleus; χ_o is the alpha internal function. The radial wave function is now characterized by a two-component vector function of r, $\begin{pmatrix} u_o \\ u_2 \end{pmatrix}$. This vector satisfies the following coupled equations in the region beyond short-ranged nuclear forces:

$$\begin{aligned} \frac{d^2u_o}{dr^2} - \frac{2m}{\hbar^2}\left(\frac{2Ze^2}{r} - Q_f\right)u_o &= K_{02}^2(r)\,u_2 \\ \frac{d^2u_2}{dr^2} - \frac{2m}{\hbar^2}\left(\frac{2Ze^2}{r} + \frac{6\hbar^2}{2mr^2} - Q_f + E_2\right)u_2 &= K_{20}^2(r)\,u_o \end{aligned} \tag{6.2}$$

where E_2 is the energy of the excited state and $\frac{6\hbar^2}{2mr^2}$ is the centrifugal energy term $\frac{\hbar^2}{2mr^2}\ell(\ell+1)$. The coupling coefficient $K^2_{02}(r)$ has been shown to be uniquely related to the reduced electric transition probability $B(E\lambda)$ between the coupled final states. This relation is given by eq. (29.14) of ref. 17, and we call attention to an error in this equation. The factor of $\lambda!$ in the denominator should be replaced by unity. Thus, quite generally

$$K^{\lambda}_{\ell I_f \ell' I'_f}(r) = (-)^{I'_f - I} \frac{2m}{\hbar^2} \frac{2e[(2\ell+1)(2\ell'+1)4\pi(2I'_f+1)B_{I'_f \to I_f}(E\lambda)]^{1/2}}{r^{\lambda+1}(2\lambda+1)} \qquad (6.3)$$

$$\times \ (\ell\ell' 00 \,|\lambda 0\,)\, W(\ell I_f\, \ell' I'_f;\, I\lambda\,)$$

For the E2 transition in the example there are $\frac{1}{r^3}$ coupling terms on the right-hand side of eq. (6.2). However, the coupling terms are likely to be stronger in the nuclear surface region where short-range nuclear forces are effective, but we do not know their form or strength nearly as well as we know the electric terms. The refinement of treating coupled equations in the region of spherical nuclei has not yet been seriously attempted. When we go on into the spheroidal nuclear region, we have a better defined model, and the non-central coupling strengths are larger. For the coupling within a rotational band, perturbation solutions are not useful for the systems of coupled radial equations. Considerable theoretical attention has been given to this problem [40,41,42,43,44].

In the region ($\geq$ 12 fm) beyond the range of nuclear forces the problem of decay to a band of a spheroidal nucleus can be rather precisely formulated in terms of a set of coupled equations of the general form of eq. (6.2). If an intraband E2 transition rate or Coulomb excitation cross section is known, the intrinsic quadrupole moment Q_o is calculable. In terms of Q_o eq. (6.3) for the coupling matrix elements may be rewritten

$$K^2_{\ell I_f \ell' I'_f\, I_i}(r) = (-)^{I_f+I'_f-K-I_i}\ \frac{2mQ_o e^2}{5\hbar^2 r^3}\left[(2I_f+1)(2I'_f+1)(2\ell+1)(2\ell'+1)\right]^{1/2} \tag{6.4}$$

$$\times\ (I_f I'_f\ K\text{-}K|20)(\ell\ell'00|20)\ W(\ell I_f \ell' I'_f;\ I_i 2)$$

where the initial spin is $\underline{I_i}$, the coupled final states have $\underline{I_f}$, ℓ, and $\underline{I'_f}$, ℓ' and $\underline{K}$ is the usual projection of total angular momentum on the symmetry axis in the daughter states. This expression for the electric quadrupole coupling term in alpha decay simplifies for ground band decay of even nuclei, where $I_i = 0$, $K=0$, $I_f=\ell$, and $I'_f=\ell$.

$$K^2_{\ell\ell' 0}(r) = \frac{2mQ_o e^2}{5\hbar^2 r^3}\left[(2\ell+1)(2\ell'+1)\right]^{1/2}\ (\ell\ell'00|20)^2 \tag{6.5}$$

Algebraic expressions for the diagonal and off-diagonal elements of eq. (6.5) are given on p. 166 of ref. 40. (See also ref. 43.)

The basic problem to be considered here first is that we are given by some internal model the radial wave function amplitudes on a spherical surface $\underline{R_x}$ near the nucleus as a vector $\begin{pmatrix} u_o \\ u_2 \\ u_L \end{pmatrix}$ in the notation of eq. (6.2). The first derivatives of the vector components are fixed by specifying behavior like irregular Coulomb functions (in practice, by taking the decreasing exponential WKB solution). With these boundary conditions we seek to integrate the coupled equations to very large distance $\underline{R_d}$ to obtain predictions of alpha decay intensities to various members of the rotational band. The intensities are given by the velocity of the partial wave times the square of its amplitude of oscillation near $\underline{R_d}$ times the surface area of the sphere $4\pi R_d^2$. Where the initial boundary conditions are on a sphere near the nucleus we indicate the argument with a subscript or R_q.

A most convenient approximation to the solution of the coupled equations is the matrix method of Fröman[41]) (similar expressions have also

been given by Nosov[42]. The basis of the approximation is the consideration that the non-central coupling terms are mainly effective near the nucleus and that the differences in effective barrier energy for the different partial waves make themselves felt mainly at larger distances. Fröman essentially solves the barrier penetration problem twice, once with non-central coupling terms included but diagonal energy differences (nuclear rotational energy and the centrifugal energy) ignored and again with coupling terms absent and diagonal energy differences included. His final solution is a product of the matrices representing solutions of the two idealized problems. Numerical integration studies[45] have showed the approximation to be rather good except in cases of rather weak partial waves coupled to relatively strong partial waves.

To apply the Fröman method we simply multiply the vector $u_j(R_x)$ by a square matrix and treat the resultant vector $w_j(R_x)$ as for barrier penetration with no coupling terms.

$$w_j = \sum_{j'} k_{jj'}(B)\, u_{j'} \tag{6.6}$$

where, for even nuclei,

$$k_{jj'}(B) = \int Y^*_{jo}(\omega)\, e^{BP_2(\cos\theta)}\, Y_{j'o}(\omega)\, d\omega \tag{6.7}$$

The argument B is given by the difference of the WKB path integrals along $\theta = \arccos\left(\frac{1}{3}\right)^{1/2} \approx 55^\circ$ and along $\theta = 0$, where θ is the polar angle of the nuclear body-fixed coordinate system with polar axis the cylindrical symmetry axis of the nucleus.

The appropriate argument B_q is found by evaluating the equation

$$B_q = \frac{\sqrt{2m}}{\hbar} \int_{R_x}^{R_t} \left[\left(\frac{2Ze^2}{r} - Q_f \right)^{1/2} - \left(\frac{2Ze^2}{r} - Q_f + \frac{Q_o e^2}{r^3} \right)^{1/2} \right] dr \qquad (6.8)$$

By expanding the second term in powers of the quadrupole potential (as does Fröman) and retaining only the first term in Q_o we readily get the formula below

$$B_q \approx - \frac{q}{6\eta_o^2} \left(\frac{2\eta_o}{k_o R_x} - 1 \right)^{1/2} \left(1 + \frac{\eta_o}{k_o R_x} \right) \qquad (6.9)$$

where we have used the notation of Mang and Rasmussen's[36] eq. (V.7), $\underline{k_o}$ and η_o being the standard Coulomb parameters, applied to the ground group, and $\underline{q}$ is a dimensionless quadrupole coupling constant

$$q = \eta_o \frac{k_o^2 Q_o}{Z} = \frac{2mk_o Q_o e^2}{\hbar^2} \qquad (6.10)$$

Substituting parameters $\underline{k_o}$ and η_o appropriate to Cm^{242} into these equations we get a simpler approximate formula (R_x = 11.1 fm, the top of the barrier with Igo's potential along $\theta = 55^o$)

$$B_q \approx - 0.045\, Q_o \qquad (6.11)$$

where $\underline{Q_o}$ is to be in units of 10^{-24} cm^2 (barns).

The numerical integration studies on Cm^{242} by Rasmussen and Hansen[45] dealt with the relation between relative intensities and the wave function on a spherical surface near the nucleus. Their work makes a direct comparison with the Fröman matrices. From the numerical integration the equivalent matrices are not completely symmetric, as is the Fröman matrix from eq. (6.7). (See also Fröman's numerical tabulation of matrix elements[41]). The asymmetry is not sufficient to affect seriously the intensity predictions for the more intense partial waves, but weak groups may be more seriously affected.

Furthermore, the matrix elements from the numerical work showed small imaginary components, representing the need to include some regular Coulomb function admixture with the dominant irregular at infinity. Nosov[42]) treated the problem analogously to Fröman. However, Nosov's formula called for a small imaginary component in the argument $\underline{B}$. Jacobsohn and Miller pointed out[46]) that the imaginary components are due to Coulomb excitation (non-resonant) processes occuring beyond the classical turning point $\underline{R_t}$. Mang and Rasmussen have reconsidered the problem[36]), giving practical formulas for applying the correction. It is better not to make the corrections by a complex argument in the main Fröman matrix but to calculate a correction matrix $\hat{k}_{\ell\ell'}$ to multiply the originally predicted wave amplitude vector beyond the barrier. A simple approximate formula, bearing close relation to Nosov's result, is as follows:

$$\hat{k}_{\ell\ell'} = \delta_{\ell\ell'} - \frac{iq}{6\eta^2} \int Y^*_{\ell' m}(\omega)\, P_2(\cos\theta)\, Y_{\ell m}(\omega)\, d\omega \qquad (6.12)$$

with $\underline{q}$ as defined by eq. (6.10), and m = 0 for decay of even nuclei to ground. The correction is only of significance for weak groups. Mang and Rasmussen noted that Coulomb excitation establishes a rigorous restriction on the minimum intensity of weak groups relative to stronger groups to which they are coupled. Using an assumed Q_o of 11×10^{-24} cm^2 and other parameters having their values for Cm^{242}, the inequality below was derived:

$$\frac{\text{Intensity } (L=4)}{\text{Intensity } (L=2)} \geq 9.5 \times 10^{-4}$$

The experimental ratio in Cm^{242} is 11.4×10^{-4}, obeying the limit, but the ratio in Cm^{244} is 7.3×10^{-4}, slightly violating the limit but within the uncertainties attached to the intensity ratio and the quadrupole moment.

The Coulomb excitation corrections also introduce a phase shift away from normal Coulomb phase for the partial waves. The phase shift is not a physically measurable quantity in the decay of spin-zero nuclei, but in odd-mass cases, where alpha groups may have mixed angular momenta, the phase shift affects the interference term in alpha angular distribution experiments.

It is of more fundamental interest to carry the alpha wave function vector on into the region of the attractive nuclear force, perhaps to a distorted surface at constant nuclear density or constant potential for the alpha. Here we must necessarily suffer some loss of rigor. Frequently the vector specifying the alpha wave function is redefined to specify a spherical harmonic expansion on a spheroidal, rather than spherical, surface. One may obtain coupled equations of the form of eq. (6.2) in a spheroidal coordinate system, but the nuclear rotational energy is then not entirely diagonal, though it is always approximated as diagonal. The numerical integrations of Rasmussen and Segall[40]) and of Pennington and Preston[44]) considered the electric potential of a uniformly-charged spheroid to carry exactly in to a spheroidal cut-off surface. Fröman's and Nosov's approximate matrix solutions also are based on the sharp cut-off picture, but they lend themselves to easy modification through changing the argument of the matrix. Mang and Rasmussen[36]) attempted to refine the analysis by assuming a diffuse nuclear potential rising linearly at any angle θ as a function only of the distance from the effective surface of a uniformly charged spheroid with the proper size and quadrupole moment. The nuclear potential abruptly ends and the potential is assumed pure Coulombic beyond a point of intersection. They give prescriptions for arguments of Fröman matrices appropriate to transmission through such a barrier.

They have gone on to apply shell-model alpha theory using Nilsson

orbitals to the calculation of relative intensities to the ground rotational band members in even-even spheroidal nuclei. The theoretical alpha wave function varies over the spheroidal nuclear surface in the same sense as an average of the wave functions of the most lightly bound neutrons and protons.

Another approach to the theory of relative alpha intensities in spheroidal nuclei begins with the assumption that the alpha wave function should be constant over the nuclear surface. Then the data are used to calculate the quadrupole, 2^4-pole, and occasionally other deformation parameters of the nuclear surface. The quadrupole deformations calculated from this approach usually gently decrease throughout the whole actinide region[41,42,43], whereas the experimental and theoretical values (cf. Szymanski[47]) generally increase. These treatments also yield negative $P_4(\cos\theta)$ terms in the deformation in the vicinity of Pu^{238}, but the Kjällqvist theoretical β_4 values are everywhere positive[48].

The existence of a unique relationship between alpha relative intensities and nuclear shape parameters is not necessarily antithetical to shell-model theory, which predicts non-uniform alpha boundary conditions over the nuclear surface. Equilibrium deformations and the shell-model alpha surface wave functions both depend on the occupied Nilsson orbitals beyond closed shells. The change in equilibrium deformation upon addition of nucleons will depend mainly on properties of orbitals near the Fermi energy (with distance less than or of the order of the "energy gap" 2Δ). Early in the filling of a major shell where the Fermi energy is in the neighborhood of strongly down-sloping orbitals in the Nilsson diagram (cf. figs. 5 and 6 of ref. 49 or figs. 1 and 2 of ref. 50) the addition of nucleons brings an increasing quadrupole distortion. Likewise, in this

region the shell-model alpha theory will yield an alpha wave function on the surface that is concentrated near the poles of the nucleus and manifests itself in a large relative intensity of decay to the first excited state. It seems reasonable that one might develop a simple modified theory relating alpha intensities to shape parameters; this theory must make the L=2 "partial wave" amplitude on the spheroidal surface proportional to the change in quadrupole deformation from daughter to parent. Likewise, the L=4 surface amplitude should be proportional to the change in β_4 which change seems to be negative throughout the region of 90 to 100 calculated by Kjällqvist[48]).

One finds the following approximate relation between the quadrupole deformation δ_α of the surface over which the alpha wave function is constant as calculated by Nosov[51]), and the δ for the surface of constant matter density from Szymanski[47]):

$$\delta_\alpha \approx \delta + 10(\delta_{parent} - \delta)$$

where the δ values apply to the daughter except for the one with the subscript parent.

With much more uncertainty one can find a similar relation for the coefficients of P_4 deformation. Taking the α_4 values for the surface of constant alpha wave function calculated by Goldin, Novikova, and Ter-Martirosyan[52]) for four even-even nuclei and comparing with the Kjällqvist theoretical deformations we have the following:

$$\sqrt{\frac{4\pi}{9}}\ \alpha_{4\alpha} = \beta_{4\alpha} = \beta + 15(\beta_{4parent} - \beta_4)$$

The coefficients of the shape-change terms are empirical and have not yet been derived theoretically. The relationships not involving nucleonic wave functions deserve further study and refinement, since they offer hope of measuring the P_4 term in the nuclear shape, a quantity apparently not measurable by other experimental techniques.

7. Decay Rates of Odd-Mass and Odd-Odd Nuclei

It was early noted that the alpha groups of odd-A nuclear types exhibited reduced widths ranging from those of even nuclei down to much smaller values. It was logical that some sort of selection rules be sought to explain this behavior.

For beta and gamma transition rates a natural scheme of classification is according to multipolarity, that is, the angular momentum associated with the radiation. For the energies encountered in radioactivity, angular momentum strongly affects beta and gamma transition rates. In the case of the emission of the massive alpha particle the centrifugal barrier inhibiting emission associated with angular momentum changes plays only a subordinate role in determining rates, and for alpha emission with parent and daughter spins exceeding 1/2 angular momentum mixtures are nearly always found when angular correlation experiments are performed on alpha radiation. The centrifugal barrier effect on penetration can be approximated for low L values by the factor

$$\left(\frac{G_L(\rho_o \eta)}{G_o(\rho_o \eta)} \right)^{-2} = \exp \left[- \frac{L(L+1)}{\eta} \left(\frac{2\eta}{\rho_o} - 1 \right)^{1/2} \right] \qquad (7.1)$$

where η is the standard argument of the Coulomb functions and ρ_o is the value of the dimensionless distance parameter $\rho (=kr)$ at the nuclear surface. For higher $\underline{L}$ values it is better to use eq. (5.13). The centrifugal factors become very small for very high L, but they change much too slowly to produce a distinct separation of decay rates according to multipolarity, and they are generally not small enough to explain alone the large hindrance factors known in many cases of $\Delta I = 0$, 1 or 2.

Instead of multipolarity Perlman, Ghiorso, and Seaborg proposed[53]) the guiding rule in alpha decay that alpha formation involving unpaired nucleons proceeds more slowly than that involving pairs. If the difference between parent and daughter wave functions is just the paired nucleon configuration and the odd-nucleon wave function remains unchanged, the decay may proceed at a rate approaching that of even nuclei. The alpha group for which this is the case usually goes to an excited state (exceptions: U^{233} and Es^{253} and several spherical nuclei), and the group is usually referred to as "favored". All other groups in a given nucleus will be hindered to some degree. A useful "rule-of-thumb" is that the strength of a given partial wave of angular momentum $\underline{L}$ to a state other than the favored will qualitatively vary as the electric 2^L-pole transition probability connecting the particular daughter state with the favored state. For example, there is only small hindrance for L=2 decay to those excited members of the favored rotational band which have very strong rotational E2 transition probabilities to the favored state. In hindered decay of Cm^{243} to the ground band we have an interesting example: the parent spin and parity are 5/2+ and the daughter Pu^{239} has 1/2+. Decay must be pure L=2 to the ground state and it is highly hindered (~5000). Decay to the 3/2+ first excited state may proceed by L=2 and L=4, and it is a factor of 5 less hindered. Experimentally, the E2 transitions from the favored state at 286-keV down to the ground band are much weaker than single particle strength. The asymptotic quantum number selection rules[49]) explain the retardation of the E2 transitions as arising from a change in intrinsic spin projection ($\Delta\Sigma = 1$) for the dominant parts of the odd-nucleon wave function. As analysis of the intensity pattern of alpha decay to six states of the Pu^{239} ground band shows, the L=4 wave is indeed stronger than L=2. Although E4 transition rates are not experimentally measurable, the asymptotic selection rules allow E4 to connect

with the favored state. For an example of the "rule-of-thumb" in the spherical region we consider the decay of Bi^{211} to the first excited state (presumably a $d_{3/2}$ proton hole) of Tl^{207}. The odd proton in Bi^{211} is $h_{9/2}$. To use the electric transition rule to guess the relative strengths of L=3 and 5 partial waves we look at the vector diagram of fig. 7.1. It is obvious that the E5 transition will be somewhat retarded by geometrical factors, since there tends to be an intrinsic-spin flip. An E3 transition proceeds with little change in intrinsic spin orientation. Shell-model alpha theoretical calculations of Mang[27]) show the L=5 admixture only 0.12 of the L=3, an admixture consistent with the alpha-gamma directional and polarization correlation experimentally observed [54]). We shall presently develop some justification for the electric transition rule. Accepting it, we may make several predictions: The L=1 partial waves will often be highly hindered, since low-energy E1 transition probabilities are greatly retarded in spherical and spheroidal nuclei. For spherical nuclei with parent and daughter orbitals of opposite type ($j_i = \ell_i \pm 1/2$, $j_f = \ell_f \mp 1/2$) the higher of the permitted $\underline{L}$ values in alpha decay are preferred, and when the orbitals are of like type, the alpha decay may go nearly purely by the lowest allowed $\underline{L}$ value. The corollary of this rule for spheroidal nuclei is that if Σ (projection of intrinsic spin) changes (as in Cm^{243} discussed above), the alpha decay will avoid $\underline{L}$ values less than $\underline{K_i} + \underline{K_f}$, ($\underline{K}$ being the familiar projection of total angular momentum) and conversely for no Σ change in the odd nucleon the lowest allowed $\underline{L}$ values tend to be favored. It is well to bear in mind that the rule is only valid on the average, and serious exceptions may be encountered. Where intrinsic spin orientation governs hindrance for electric transitions, the hindrance more generally will carry over to alpha decay, but where a cancellation in angular or radial orbital integrals is involved, alpha decay rates may depart from the rule, since two

kinds of nucleons are involved in alpha decay.

Prior has made a correlation [55]) of hindrance factors F (calculated by a formula due to Fröman[41])) for odd-A nuclei. He sought relationships between F and the changes in asymptotic quantum numbers in the orbital of the odd-nucleon. He treated only decay groups to the lowest state of rotational bands and summarized his observations as follows:

a. The favored transitions mostly have F between 1 and 4.

b. There are some transitions in a region of F between 8 and 20 including some favored decay and some to levels containing favored state configuration mixture through the Coriolis interaction.

c. All transitions with $F > 630$ have a spin flip $\Delta\Sigma = \pm 1$.

d. The transitions involving a change in parity and no spin flip have F between 60 and 600.

Prior's observations are clearly consistent with the electric transition rule.

It is in the calculation of relative alpha intensities for Po^{211} decay that the shell-model alpha theory has enjoyed striking successes. The decay scheme of Po^{211} is shown in fig. 7.2.

It is of interest to carry out these ratio calculations by the simple delta-function model. Equations (5.28) and (5.29) were given for favored and hindered decay of even-even nuclei to or from closed shell configurations. By use of fractional parentage coefficients these equations may be used away from closed shells and with odd-A nuclei. For Po^{211} the fractional parentage coefficients will be unity. After a Racah recoupling of three angular momenta (most easily done by second quantization methods) to project out the appropriate configuration with attention to antisymmetrization, eq. (5.29) can be directly applied. For decay from one-odd-nucleon to one-hole nuclei there comes an extra factor of $\left(\frac{2L+1}{2j_i+1}\right)^{1/2}$, where j_i is the angular momentum of the initial

state orbital.

For Po^{211}, which decays across the 126-neutron shell, the alphas to the Pb^{207} final states are formed from the odd $g_{9/2}$ neutron and one of a pair of neutrons in orbit $j'(p_{1/2}, f_{5/2}, \text{ or } p_{3/2})$. If we wish only to calculate alpha reduced widths relative to the ground state transition, the factors depending on the paired proton orbitals divide out. Let us designate the $p_{1/2}$ Pb^{207} ground state A, the $f_{5/2}$ first-excited state B, and the $p_{3/2}$ second excited state C. Remembering that the alpha formation proceeds from a $g_{9/2}$ neutron plus one from the final state orbital we have

$$\frac{\gamma_{L\, j'}}{\gamma_{5\, p_{1/2}}} = \left[\frac{(2j'+1)}{2}\right]^{1/2} \frac{(j'\ \frac{9}{2}\ \frac{1}{2}\ -\frac{1}{2} \mid L0)}{(\frac{1}{2}\ \frac{9}{2}\ \frac{1}{2}\ -\frac{1}{2} \mid 50)} \cdot \frac{R'_j}{R_{p_{1/2}}} \cdot \frac{B_n(\ell_f\ \ell_i\ L)}{B_n(1\ \ell_i\ L)} \tag{7.2}$$

Table 7.1 shows the results of the calculations with eq. (7.2). After calculation of reduced widths γ^2, using Blomqvist-Wahlborn radial functions[34] at 9 fm, they are further multiplied by relative barrier penetrability factors[21] to facilitate comparison with experiment and with previous theoretical calculations of Zeh and Mang[31].

Table 7.1

Theoretical Relative Alpha Intensities for Po^{211}

Pb^{207} final state	L	Angular factors ratio	Radial function ratio (R_o = 9 fm)	Finite alpha correction ($B_f/B_{1/2}$)	$\frac{\gamma_j}{\gamma_{p_{1/2}}}$	Relative intensities		
						Eq. (7.2)	Finite alpha theory (Zeh-Mang[31])	Experiment
A ($p_{1/2}$)	5	1	1	1	1	10^4	10^4	10^4
B ($f_{5/2}$)	3	0.427	0.74	0.883	0.279	44	37	24
	5	-0.785	0.74	0.938	-0.545	39	30	22
	7	1.49	0.74	1.020	1.124	19	13	~ 7
Total to B						102	80	53
C ($p_{3/2}$)	3	-1.16	1.0	0.942	-1.092	43	44	49
	5	0.816	1.0	1.00	0.816	6	5	1?
Total to C						49	49	50

To calculate relative alpha intensities further from closed shells using eq. (5.29) it may be necessary to multiply by a correction factor from pairing force calculations. That is, the square of the matrix element should be multiplied by the probability that the final orbital of the odd nucleon is occupied by a pair in the parent times the probability that the initial orbital of the odd nucleon is vacant in the daughter.

The principal angular factors in eq. (5.29) for the relative reduced alpha widths of unfavored decay of angular momentum $\underline{L}$ are identical to the statistical factor in the Weisskopf electric-transition-probability formula. $S(j_i j_f L)$ for the electric 2^L-pole radiation formula. It has been pointed out[33] that the usual form of the S-factor involving a Racah coefficient can be simplified to a Clebsh-Gordan form like eq. (5.29).

We see the qualitative operation of the "electric transition rule" from examination of the $\gamma_j/\gamma_{p_{1/2}}$ column. For the $f_{5/2}$ final state B, (a $j = \ell - 1/2$ orbital whereas the $g_{9/2}$ initial orbital is of $\ell + 1/2$ type) the high angular momenta are favored intrinsically. For the $p_{3/2}$ final state, C, the opposite holds.

In deformed nuclei for non-zero parent spin Bohr, Fröman, and Mottelson[56] advanced some very useful branching relations governing relative intensities of decay to different states of a rotational band. The projection $\underline{K}$ of total angular momentum along the nuclear symmetry axis is nearly a constant of the motion for most spheroidal nuclei. Thus, one expects that the conservation laws will force the projection of alpha orbital angular momentum $\underline{m_L}$ to add with the daughter $\underline{K_f}$ (or $-\underline{K_f}$) to equal the parent $\underline{K_i}$, at least for alpha separation distances not far from the nucleus. To satisfy this condition a given partial wave $\underline{L}$ must split into components to various final rotational states in the ratio of Clebsch-Gordan coefficients. In subsequent

transmission through the barrier the waves to different final states will suffer different attenuation according to the Gamow penetrability factor (reciprocal square of the irregular Coulomb function at $\underline{R_o}$) for each. Thus, we have the formula for the partial decay constants to a band.

$$\lambda_{LI_f} = \frac{v_L}{R_o} P_L(E_f) \left| (-)^{I_f+K_f} b_L(I_i L K_i K_f - K_i | I_f K_f) + b'_L(I_i L K_i - K_f - K_i | I_f - K_f) \right|^2 \quad (7.3)$$

The second term vanishes except for $L \geq K_i + K_f$ and corresponds to transitions where the angular momentum projection of the daughter nucleus is opposite from that of the parent. The $\underline{b_L}$ and $\underline{b'_L}$ are reduced wave amplitudes. The equation should be exact in the limit of infinite nuclear moment of inertia or vanishing nuclear electric quadrupole moment[57]). Actually it is an approximate relation which may be poor for weak partial waves coupled by E2 Coulomb excitation matrix elements to relatively strong partial waves.

Equation (7.3) has been most widely used to analyze the intensity patterns in decay to the favored band in odd-A nuclei. Frequently in such cases $\underline{b_L^2}$ is normalized and approximated as the reciprocal reduced hindrance factor averaged from the nearest even-even neighbors, and b'_L is taken as zero for favored decay. Table 7.3 gives such an anlysis for the Es^{253} favored band[58]).

Table 7.3

Analysis of Es^{253} Decay to the Favored Band

Excited state energy (keV)	Calculated abundances (%) (BFM approx)						Experimental values (%)
	I	Barrier penetration factor ratio	L = 0	L = 2	L = 4	Total	
0	$\frac{7}{2}$	1.00	79.6	10.0	0.127	89.7	90
41.7	$\frac{9}{2}$	0.653	--	5.92	0.327	6.24	6.6[a])
93.4	$\frac{11}{2}$	0.381	--	0.88	0.267	1.15	0.85
156	$\frac{13}{2}$	0.197	--	--	0.083	0.083	0.08
230	$\frac{15}{2}$	0.087	--	--	0.0083	0.0083	0.012

a) This intensity may be a fraction of a percent too high, since it is only partially resolved from a neighboring group.

Such analyses have been made for numerous favored decays. The agreement with experiment is generally quite good. When one looks at finer details, though, the experimental ratio of reduced transition rate to the I_o+2 level relative to that to the I_o+1 level runs lower than theory by about 20 percent in most cases. Both these groups are predominantly populated by L=2 waves, so the reduced transition ratio comes mainly from geometric considerations and equals $(I_o\ 2\ I_o\ 0 |\ I_o+2\ I_o)^2 / (I_o\ 2\ I_o\ 0 |\ I_o+1\ I_o)^2$. Detailed examination of the coupled barrier-penetrability equations with a nuclear electric quadrupole field have shown that deviation from the above ratio is to be expected with a sense dependent on the phase difference between L=0 and L=2 waves [57,59]). The observed deviation implies that L=0 and L=2 are in-phase in the main group, where they give rise to true interference effects in angular correlations. The deviations from the simple branching relations are especially large in Pu^{239} decay and are not understood.

Angular correlation experiments may test the alpha partial wave mixtures and phases inferred from the intensity pattern. In particular the predicted L=2 admixture in the main alpha group (mostly L=0) gives a large interference term seen in alpha-gamma angular correlation experiments[60,61] on Am^{241} and Am^{243} and in low-temperature-nuclear-alignment experiments[62] on Cf^{249} and Es^{253} (Np^{237} has also been studied[63]) but is somewhat more complex to interpret). In all the α-γ experiments there remains some uncertainty that the full anisotropy was observed, but in Am^{243} Asaro and Siegbahn[61]) have restored the usually-attenuated correlation by a 12 kilogauss field along the alpha direction with the recoil atoms in a vacuum. Their anisotropy requires a slightly larger admixture of L=2 with the dominant L=0 group than eq. (7.2) indicates, a deviation in accord with the expected corrections. All the experiments call for a positive δ_{02} in the dominant 0-2 interference term; that is, these waves interfere constructively along the nuclear spin axis, hence in the polar regions of the prolate spheroidal surface. The observation qualitatively confirms the original predictions of Hill and Wheeler[64]) about preference of alpha decay for the thinner barrier in the polar regions. The detailed calculations[36]) based on Nilsson nucleonic wave functions also predict this sign throughout the known heavy region; from this work we might expect that heavy nuclei far beyond the known region, where the Nilsson orbitals at the Fermi surface were predominantly up-sloping, might give S- and D-waves out-of-phase.

The quadrupole coupling effects that lead to the ~20% deviations from Clebsch-Gordan branching relations for L=2 waves are expected to be more severe for the weak L=4 groups. Data are sparse; however, in U^{233} and Es^{253} there are measurements on intensities of favored decay to the states of spin $I_o + 3$ and $I_o + 4$ (4th and 5th rotational levels), and it is fair to assume that the

L=6 admixture is negligible relative to L=4. The reduced intensity ratio should theoretically be $(I_o\ 4\ I_o\ 0 \mid I_o{+}4\ I_o)^2 / (I_o\ 4\ I_o\ 0 \mid I_o{+}3\ I_o)^2$. The deviations from theory are larger. The experimental ratio for U^{233} seems smaller than this, and the ratio for Es^{253} (Table 7.3) is larger. The senses of the deviations imply that the L=4 group is in phase with L=2 for U^{233} and is out of phase for Es^{253}. Such a conclusion is consistent with the theoretical calculations[36]) of favored decay from Nilsson wave functions; the theory predicts L=4 in-phase below its minimum intensity region around mass 244 and out-of-phase above mass 244.

Angular correlation experiments on alpha groups other than the main one might test the sign of the δ_{24} interference term.

Equation (7.3) can also be used to analyze relative intensity patterns in hindered decay to rotational bands. Here, there is no guide from even-even decay as to the values of b_L and b'_L, but they may be taken as adjustable parameters and where there are more experimental intensities than parameters, checks on the theory are possible. Asaro et al. analyzed[65]) the ground band hindered decay of Cm^{243} and related the observed alternating intensity pattern to successive band members to the interference of the two L=4 terms of eq. (7.3). The electric transition rule favors $m_L = 3$, which is the dominant term, but the asymptotic selection rule is not too good here, since the $m_L = 2$ is only slightly weaker. The L=2 group violates the asymptotic selection rules of the electric transition rule and is quite weak. The possible L=0 decay would violate the K selection rule, and it not even detectable in the analysis.

The methods of shell-model alpha rate theory can be applied to hindered decay to give quantitative comparisons with observed intensity patterns and to predict multipole admixtures. Mang, Poggenburg, and Rasmussen have

treated[66]) the ground-band decay of Cm^{243}. Nilsson's wave functions for the neutrons in the initial and final odd orbitals are used, and proton functions in ten orbitals near the Fermi surface are brought in with weighting according to the pairing-force superfluid model. The alpha wave function on the nuclear surface is transformed to that outside the barrier by multiplication by Fröman matrices and then re-expanded from the body-fixed to the space-fixed coordinate system by a Clebsch-Gordan expansion. Table 7.4 summarizes the results expressed as the ratio of the reduced widths in Cm^{243} to that of the ground transition of Cm^{244}. Thus, these entries are essentially reciprocals of hindrance factors. The reduced widths are based on penetrability factors for L=0; hence, the different partial-wave widths for each alpha group can simply be summed. The general agreement of shell-model theory with experiment seems good. Such studies of hindered decay offer the hope of detailed testing of Nilsson wave functions of the unpaired nucleons.

Table 7.4

Shell-model Theoretical Reduced Widths for Ground Band Hindered Decay of Cm^{243}

Final state spin	Theoretical reduced width ratio $\gamma^2/\gamma^2_{Cm^{244}}$ (X10^4)				Experiment total
	L = 2	4	6	Total	
$\frac{1}{2}$	2.3	--	--	2.3	3.8
$\frac{3}{2}$	2.7	18	--	21	20
$\frac{5}{2}$	1.5	14	--	15	6.5
$\frac{7}{2}$	0.5	44	5	49	54
$\frac{9}{2}$	0.04	3.6	10	14	2.6
$\frac{11}{2}$	--	7.5	16	24	18

Soloviev[67]) has focussed attention on the specific role of superfluid properties in alpha hindrance factors. The alpha decay rates may be one of the most sensitive properties to test the clustering implicit in the configuration mixing caused by the pairing force.

References

1) E. K. Hyde and G. T. Seaborg, Handbuch der Physik vol. 42, Springer, Berlin (1957) 205

2) Everling, König, Mattauch, and Wapstra, Nuclear Physics 18 (1960) 529

3) G. Gamow, Zeits f. Physik 51 (1928) 204.

4) E. U. Condon and R. W. Gurney, Nature 122 (1928) 439.

5) J. O. Rasmussen, Revs. Modern Physics 30 (1958) 424

6) R. G. Thomas, Prog. Theo. Phys. 12 (1954) 253

7) R. D. Macfarlane and T. P. Kohman, Phys. Rev. 121 (1961) 1758

8) B. R. Mottelson and S. G. Nilsson, Mat. Fys. Skr. Dan. Vid. Selsk 1 (1959) no. 8

9) Stephens, Asaro, and Perlman, Phys. Rev. 113 (1959) 212

10) R. D. Macfarlane and I. Almodovar, Phys. Rev. 127 (1962) 1665

11) H. A. Bethe, Revs. Modern Phys. 9 (1937) 69. cf. p. 170

12) J. O. Rasmussen, UCRL-10414, Nuclear Physics (to be published)

13) G. H. Briggs, Revs. Modern Physics 26 (1954) 1

14) C. P. Browne, Phys. Rev. 126 (1962) 1139

15) G. Bastin-Scoffier and M. R. J. Walen, J. Phys. radium 19 (1958) 527

16) R. Taagepera and M. Nurmia, Ann. Acad. Sci. Fennicae, Ser. A. VI, No. 78 (1961) 1

17) I. Perlman and J. O. Rasmussen, chapter on "Alpha Radioactivity" in Handbuch der Physik, vol. 42, Springer, Berlin (1957) 109

18) cf. G. H. Winslow, Phys. Rev. 96 (1954) 1032

19) G. H. Winslow, On the One-Body Model of Alpha Radioactivity IV, Argonne National Laboratory Report ANL-5381, Jan., 1955, (unpublished). cf. also ref. 17

20) G. Igo, Phys. Rev. 115 (1959) 1665

21) J. O. Rasmussen, Phys. Rev. 113 (1959) 1593; Phys. Rev. 115 (1959) 1675

22) M. Born, Zeits.f. Physik 58 (1929) 306

23) S. Biswas and J. Patro, Indian J. Phys. 22 (1948) 540;
I. Perlman and T. J. Ypsilantis, Phys. Rev. 79 (1950) 30

24) cf. M. A. Preston, Physics of the Nucleus, Addison-Wesley (1962) Ch. 3

25) C. E. Fröberg, Revs. Modern Physics 27 (1955) 399

26) H. Casimir, Physica 1 (1934) 193

27) H. J. Mang, Zeits f. Physik 148 (1957) 572, Sitzungsberichte der Heidelberger Akademie der Wissenschaften (1959) 299

28) M. A. Preston, Phys. Rev. 71 (1947) 865

29) I. Kaplan, Phys. Rev. 81 (1951) 962

30) H. J. Mang, Phys. Rev. 119 (1960) 1069

31) H. D. Zeh and H. J. Mang, Nuclear Physics 29 (1962) 529

32) P. J. Brussaard and H. A. Tolhoek, Physica 24 (1958) 263

33) cf. Brody, Jacob and Moshinsky, Nuclear Physics 17 (1960) 16

34) J. Blomqvist and S. Wahlborn, Arkiv för Fysik 16 (1960) 545

35) K. Harada, Prog. Theo. Phys. 26 (1961) 667

36) H. J. Mang and J. O. Rasmussen, Mat. Fys. Skr. Dan. Vid. Selsk. 2 (1962) no. 3

37) H. D. Zeh, Dissertation, University of Heidelberg (1961) unpublished

38) D. H. Wilkinson, Proc. of the Rutherford Conf. on Nuclear Structure, (1961) 339

39) M. A. Preston, Phys. Rev. 75 (1949) 90

40) J. O. Rasmussen and B. Segall, Phys. Rev. 103 (1956) 1298

41) P. O. Fröman, Mat. Fys. Skr. Dan. Vid. Selsk. 1 (1957) no. 3

42) V. G. Nosov, Dokl. Akad. Nauk. S. S. S. R. 112 (1957) 414

43) V. M. Strutinsky, Zh. Eksp i Teor. Fiz. 32 (1957) 1412; Gol'din, Adel'son-Velskii, Birzgal, Piliia, and Ter-Martirosyan, Zh. Eksp i Teor. Fiz. 35 (1959) 184

44) E. M. Pennington and M. A. Preston, Canad. J. Phys. 36 (1958) 944; R. R. Chasman and J. O. Rasmussen, Phys. Rev. 112 (1958) 512

45) J. O. Rasmussen and E. R. Hansen, Phys. Rev. 109 (1958) 1656

46) B. A. Jacobsohn and L. W. Miller, Compt. rend. du Congres International de Phys. Nuc.; Dunod, Paris (1959) 900

47) Z. Szymanski, Nuclear Physics 28 (1961) 63

48) K. Kjällqvist, Nuclear Physics 9 (1958) 163

49) B. R. Mottelson and S. G. Nilsson, Mat. Fys. Skr. Dan. Vid. Selsk. 1 (1959) no. 8

50) Stephens, Asaro, and Perlman, Phys. Rev. 113 (1959) 212

51) V. G. Nosov, Zh. Eksp. i Teor. Fiz. 37 (1959) 884

52) L. L. Gol'din, G. I. Novikova, and K. A. Ter-Martirosyan, Zh. Eksp. i Teor. Fiz. 36 (1959) 512

53) Perlman, Ghiorso, and Seaborg, Phys. Rev. 77 (1950) 26

54) Gorodetzky, Beck, Knipper, Manquenouille, and Richert, Compt. rend. 254 (1962) 2319

55) O. Prior, Arkiv för Fysik 16 (1959) 15

56) Bohr, Fröman, and Mottelson, Mat. Fys. Medd. Dan. Vid. Selsk. 29 (1955) no. 10

57) J. O. Rasmussen, Bull. Am. Phys. Soc. Ser. II 6 (1961) 232

58) Asaro, Thompson, Stephens, and Perlman, Proc. Int. Conf. Nuc. Structure, Kingston, Canada, (1960) 581

59) R. R. Chasman and J. O. Rasmussen, Phys. Rev. 115 (1959) 1257

60) V. E. Krohn, T. B. Novey, and S. Raboy, Phys. Rev. 105 (1957) 234

61) K. Siegbahn and F. Asaro, Physics Letters 2 (1962) 323

62) Navarro, Rasmussen and Shirley, Physics Letters 2 (1962) 353

63) Hanauer, Dabbs, Roberts, and Parker, Phys. Rev. 124 (1961) 1512

64) D. L. Hill and J. A. Wheeler, Phys. Rev. 89 (1953) 1102

65) Asaro, Thompson, Stephens, and Perlman, Bull. Am. Phys. Soc. Ser. II 2 (1957) 393

66) H. J. Mang, K. Poggenburg, and J. O. Rasmussen (unpublished results) 1963

67) V. G. Soloviev, Physics Letters 1 (1962) 202

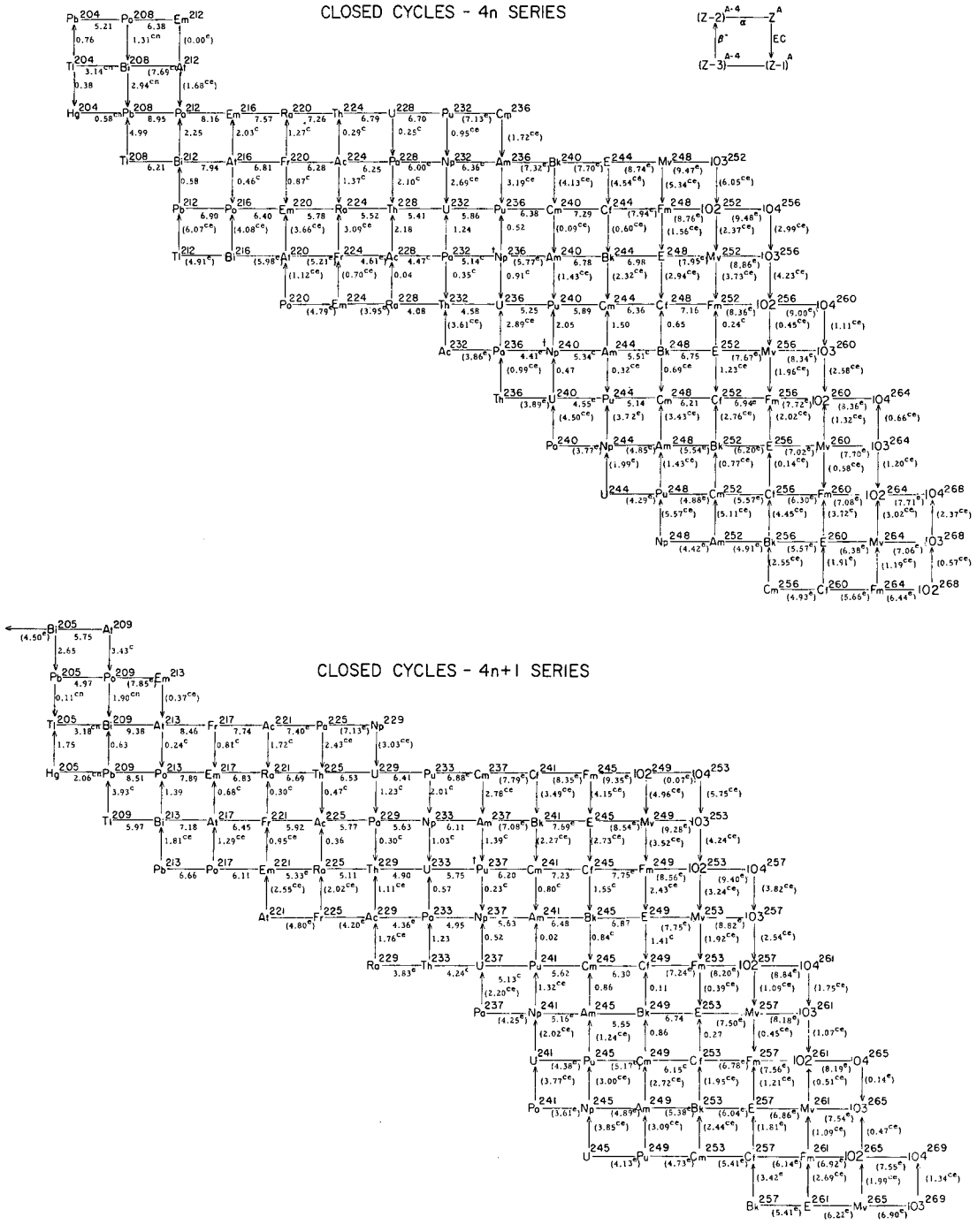

Fig. 3.1. Closed decay energy cycles for the 4n and 4n +1 series: No superscript, measured energy; c, calculated; cn, calculated with neutron binding energies; e, estimated; ce, calculated from a cycle containing estimated energies; ( ), uncertain by more than about 0.1 MeV; †, isomers.

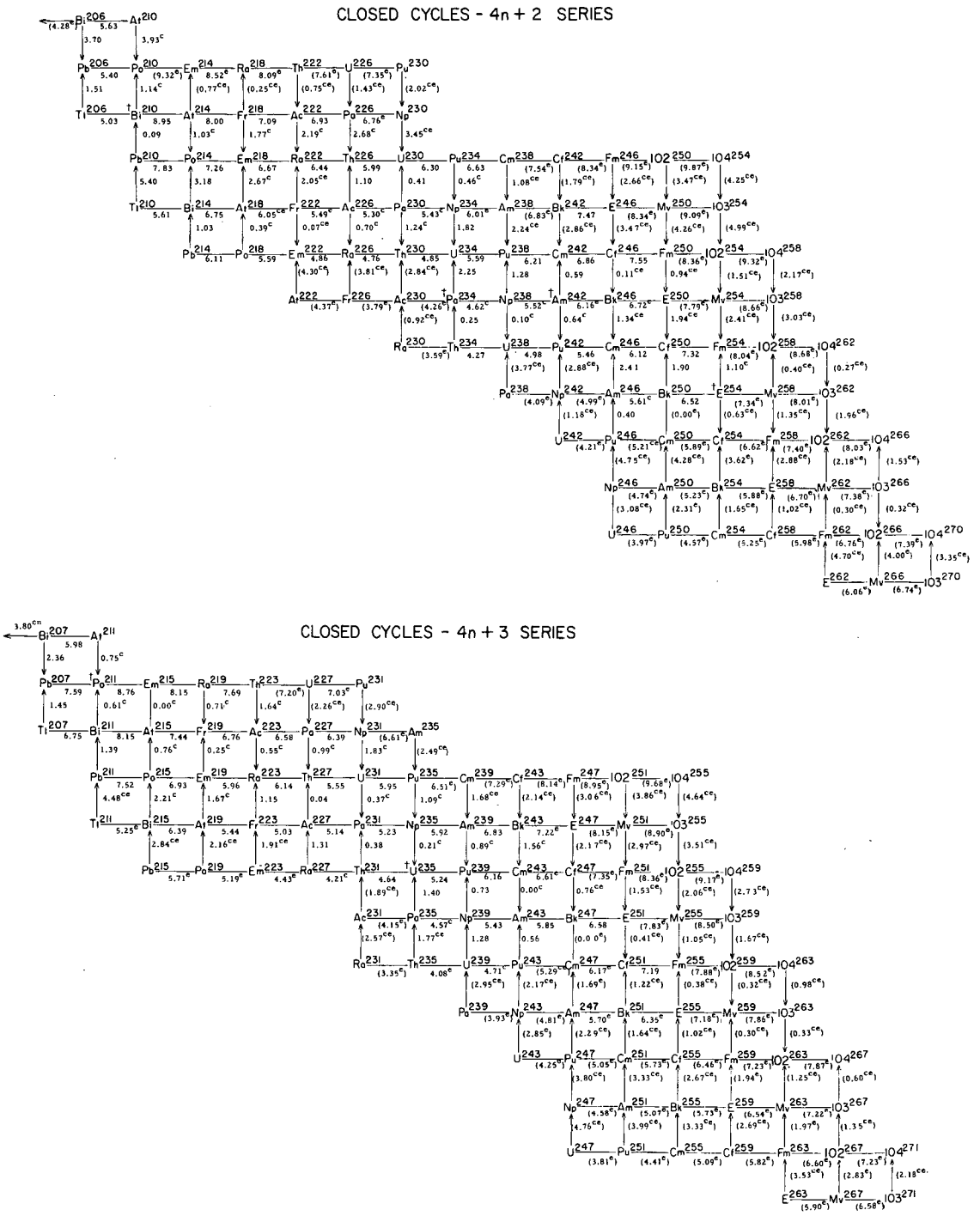

Fig. 3.2. Closed decay energy cycles for the 4n + 2 and 4n + 3 series: No superscript, measured energy; c, calculated; cn, calculated with neutron binding energies; e, estimated; ce, calculated from a cycle containing estimated energies; ( ), uncertain by more than about 0.1 MeV; †, isomers.

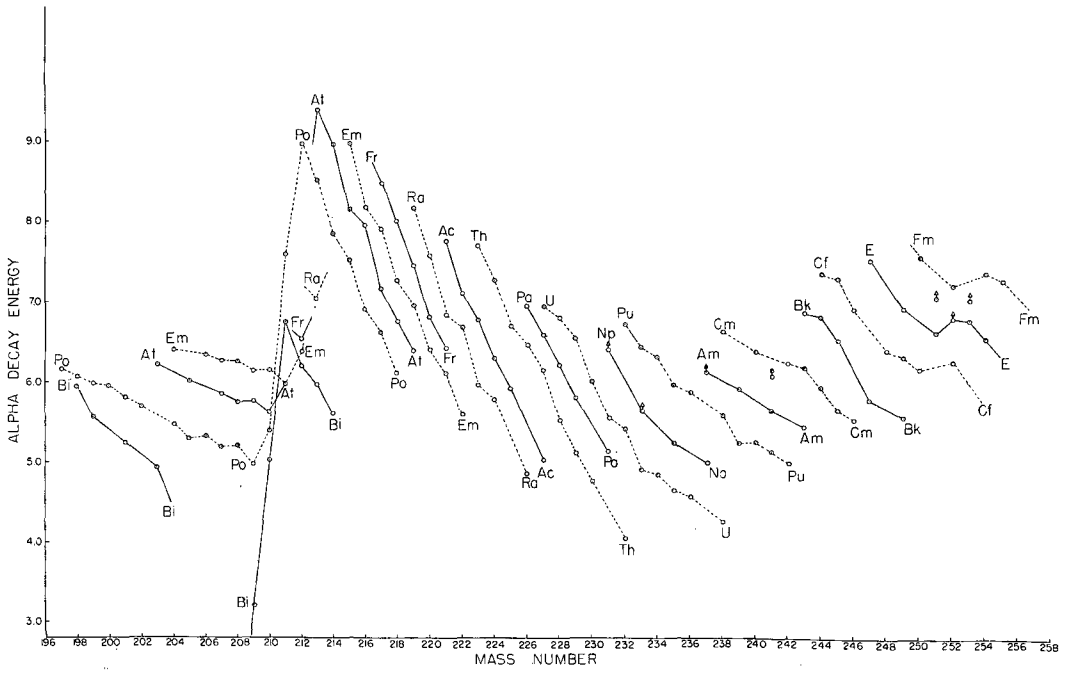

Fig. 3.3. Alpha Decay Energy Q_α (MeV) vs mass number for the region Z > 82. Points for isotopes of even-Z elements are joined by dashed lines and those for odd-Z by solid lines.

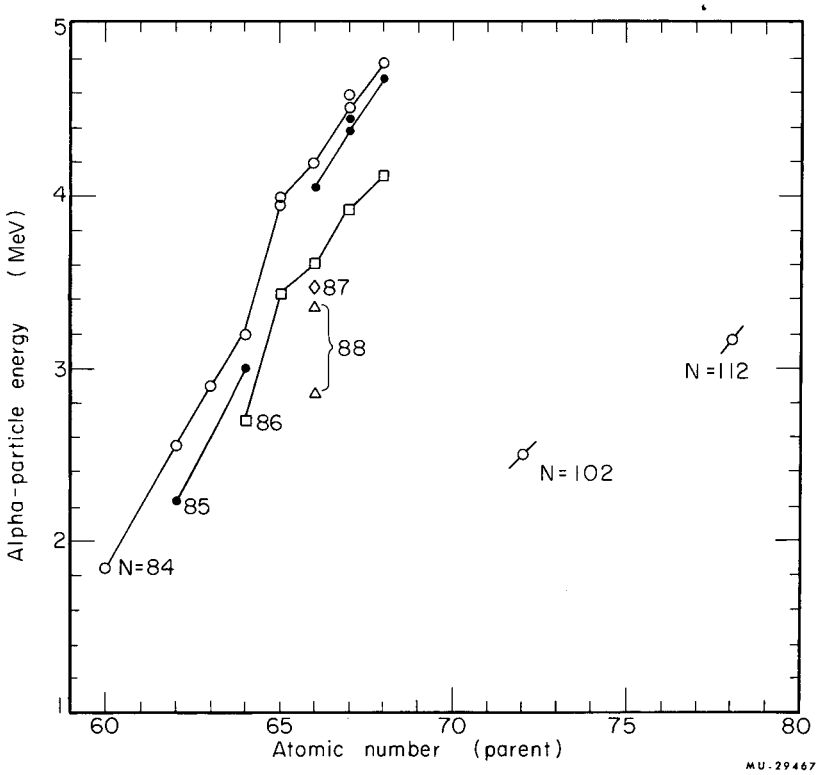

Fig. 3.4. Alpha Particle Energy E_α(MeV) vs atomic number for the region $Z < 82$. Points for isotones are joined by lines. (○ N = 84, ◐ N = 85, □ N = 86, ◇ = 87, △ = 88)

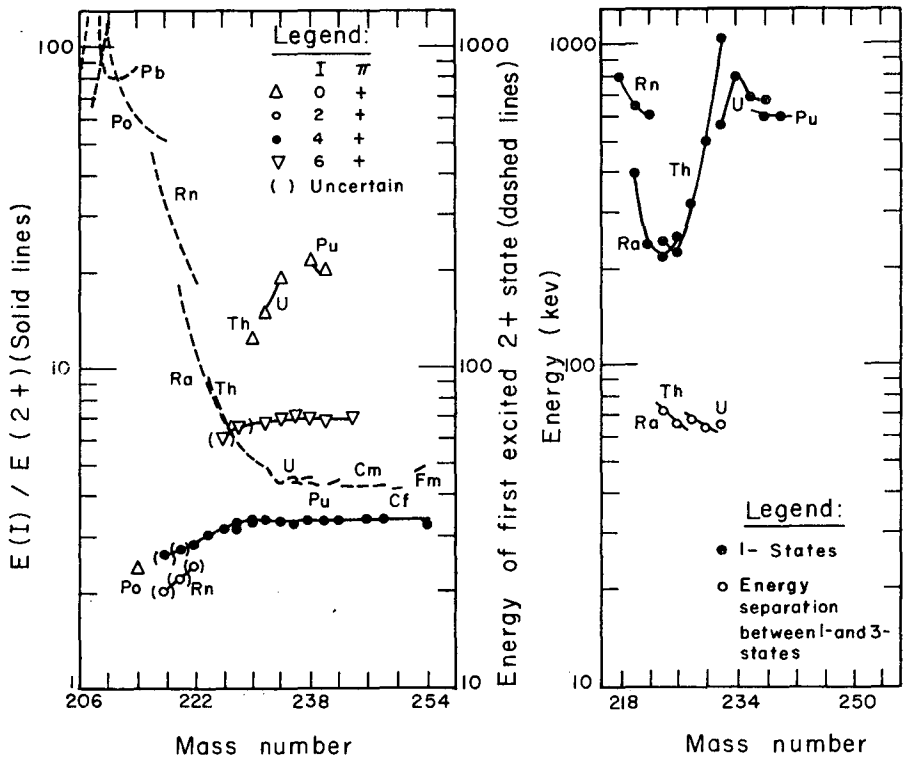

Fig. 3.5. Energy levels in even-even nuclides:
a. Even spin and parity levels.
b. Odd spin and parity levels.

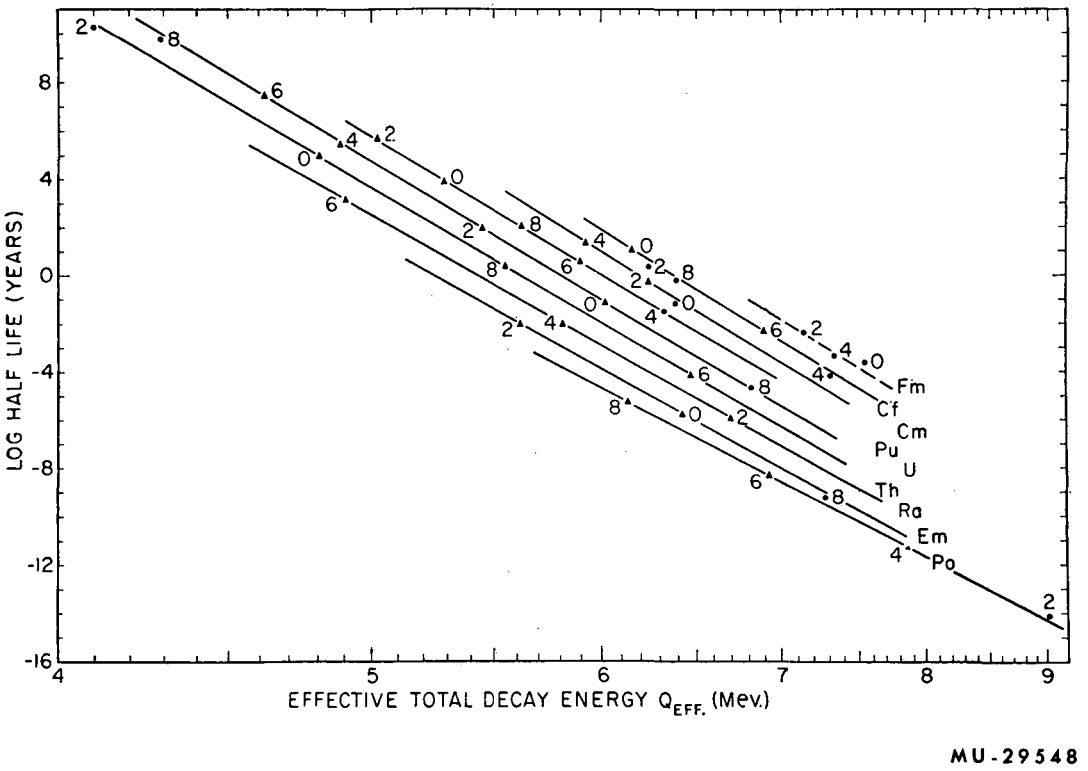

Fig. 4.1. Relation of alpha half-lives and decay energies for even-even nuclei. The abscissa is the inverse square root of the decay energy. The figure is taken from C. J. Gallagher and J. O. Rasmussen, J. Inorg. Nucl. Chem. 3 (1957) 333.

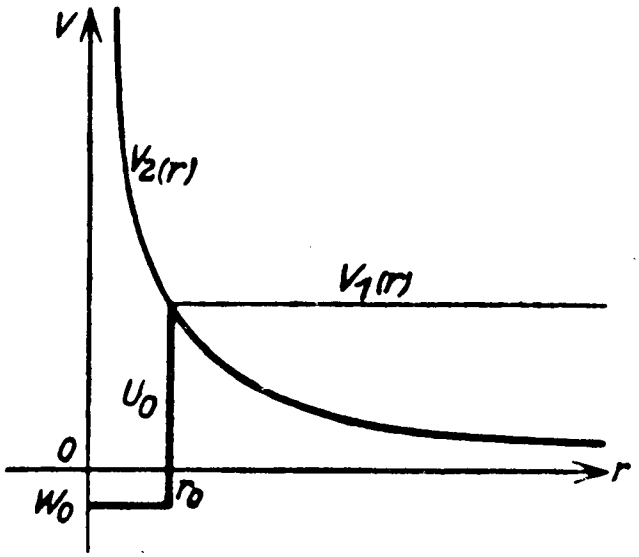

Fig. 5.1. Plot of the potentials in the Born perturbation solution to the alpha decay rate problem. V_f is the actual Coulomb potential experienced by the alpha particle V_i is the correct potential for the alpha particle for distances shorter than R_o but is an artificially-assumed potential beyond R_o, forming a real bound state. The figure is from Born's original paper[22]).

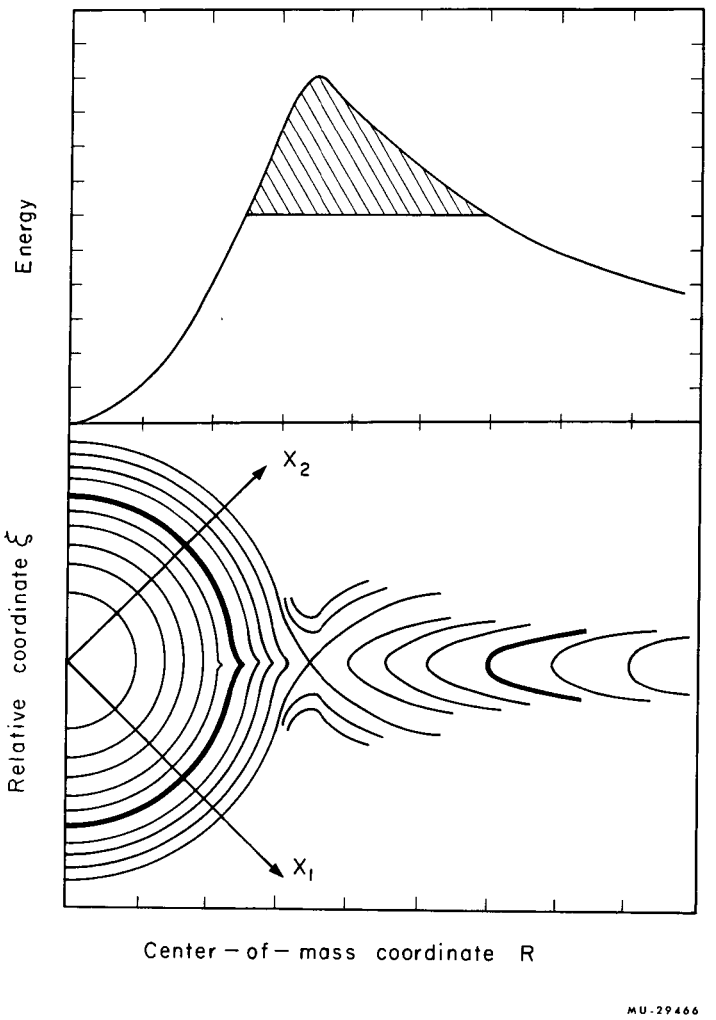

Fig. 5.2. Contour diagram of potential energy in a two-particle barrier penetration problem and a section along the valley $x_1 = x_2$. x_1 and x_2 are position coordinates of particles 1 and 2; R is the center-of-mass position coördinate and ξ is the separation distance coördinate.

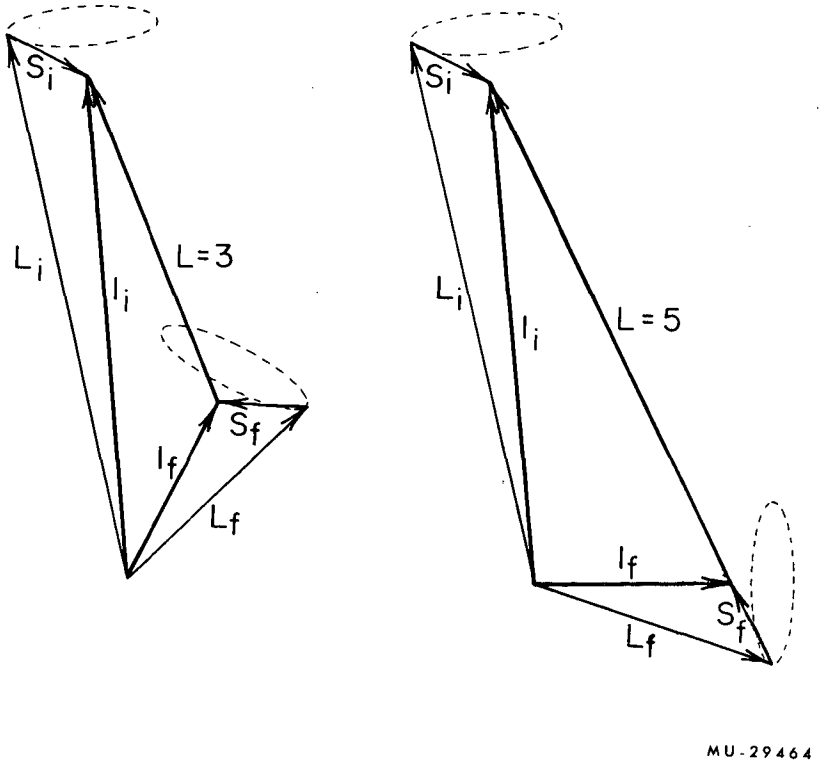

Fig. 7.1. Angular momentum relationships for E3 and E5 transitions of an odd proton from an $h_{9/2}$ to $d_{3/2}$ state. Note that the direction of the intrinsic spin must change more in E5 than E3.

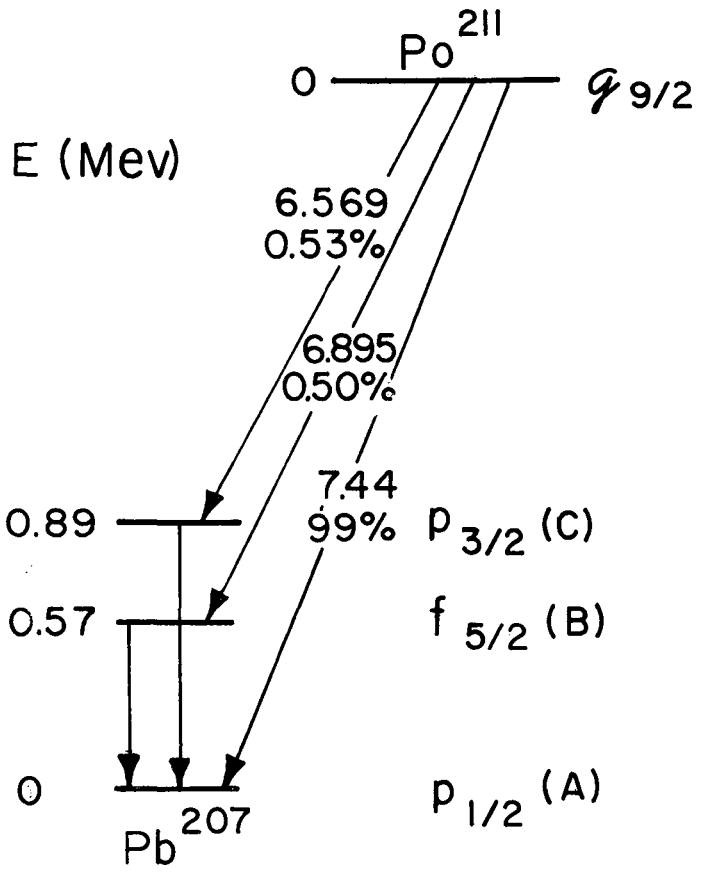

Fig. 7.2. Decay scheme of Po^{211} with shell model assignments for the odd neutron (or hole) indicated.